UPTEC X 08 013
Examensarbete 20 p
Februari 2008

Asymmetrical flow field-flow fractionation system parameters and its use on optimized quantitative antibody separation

Per Jungnelius

UPPSALA UNIVERSITET

Molecular Biotechnology Programme

Uppsala University School of Engineering

UPTEC X 08 013	**Date of issue 2008-02**

Author

Per Jungnelius

Title (English)

Asymmetrical flow field-flow fractionation system parameters and its use on optimized quantitative antibody separation

Title (Swedish)

Abstract

Method development parameters for the novel separation method asymmetrical flow field-flow fractionation were investigated and evaluated using design of experiments methodology. An optimized method for separation of immunoglobulin G aggregates was developed and results were correlated with size-exclusion high performance liquid chromatography, sedimentation velocity analytical ultracentrifugation, native polyacrylamide gel-electrophoresis and dynamic light scattering.

Keywords

A4F, FFF, method development, IgG, SE-HPLC, SV-AUC, native PAGE, DLS, DoE.

Supervisors

Michael Wouda, M.Sc.
Analytical Sciences, Biovitrum AB, Stockholm

Scientific reviewer

Prof. Karin Caldwell
Dept. of Surface Biotechnology, Uppsala University

Project name	Sponsors
Language **English**	Security
ISSN 1401-2138	Classification
Supplementary bibliographical information	Pages **58**

Biology Education Centre Biomedical Center Husargatan 3 Uppsala
Box 592 S-75124 Uppsala Tel +46 (0)18 4710000 Fax +46 (0)18 555217

Asymmetrical flow field-flow fractionation system parameters and its use on optimized quantitative antibody separation

Per Jungnelius

Sammanfattning

Asymmetrisk flödesfältflödesfraktionering är en analysteknik för att separera proteiner och andra makromolekyler med avseende på storlek. Tekniken har nyligen fått ett uppsving i samband med ökade myndighetskrav inom dess användningsområde samt att kommersiella produktlösningar nyss kommit ut på marknaden.

Separationen i asymmetrisk flödesfältflödesfraktionering sker i en tunn vätskefylld kanal. Provet tillsätts i början av kanalen och ansamlas mot ena väggen av ett tvärflöde som, i motsats till provet, kan lämna kanalen genom att ena kanalväggen är halvgenomsläpplig. Det ansamlade provet diffunderar beroende på storlek olika snabbt upp från ansamlingsväggen. Vätskeflödet som går längs med kanalen är snabbare i mitten än vid väggen och därmed kommer mindre molekyler, med högre diffusionshastighet, ut före större molekyler.

Då detta är en ny teknik på Biovitrum utvärderas här vilka inställningar som är viktigast vid framtagning av separationsmetoder. En metod för analys av antikroppar tas också fram och optimeras. Resultat från asymmetrisk flödesfältflödesfraktionering jämförs även med resultat erhållna med andra tekniker inom samma område.

Examensarbete 20p
Civilingenjörsprogrammet Molekylär bioteknik
Uppsala universitet februari 2008

Executive Summary

The new analysis technique Asymmetrical Flow Field-Flow Fractionation, A4F, has the potential to transform the field of protein aggregation analysis. The technique complements and adds to the results of today's standard technique Size-Exclusion High Performance Liquid Chromatography, SE-HPLC, and the expensive Sedimentation Velocity Analytical Ultracentrifugation, SV-AUC. In this study A4F method development parameters were evaluated using the experimental framework Design of Experiments, DoE, methodology.

During the evaluation a sample consisting of a mix of IgG antibodies induced, by UV irradiation, to contain measurable levels of covalently linked aggregates was used.

The study demonstrated that the most important method development parameter regarding selectivity was the crossflow to channel flow ratio. Other factors influencing selectivity were the channel flow rate, the use of a crossflow gradient and also the sample load.

Building on results from the DoE study, an optimized method to determine the relative amount of aggregates in the above mentioned antibody sample was developed. The method was able to separate monomers from dimers and low molecular weight impurities. The optimized method has been successfully tested for sequential runs and were shown to be robust. Both the single run and the sequence run variant is outlined in Tables 1 and 2.

Correlation studies comparing the optimized A4F method with a qualified SE-HPLC method showed that A4F measured a higher amount of aggregates when analyzing the sample. A previous study with a different sample preparation indicates that SV-AUC measures an even higher amount of aggregates. The native PolyAcrylamide Gel Electrophoresis method, native PAGE, as well as Dynamic Light Scattering, DLS, employed in this study was due to lack of resolution not fit to estimate monomer/dimer-levels for this mix of antibodies.

The study demonstrates further that the technique was informative, especially when coupled to a combination of Ultraviolet, UV, Refractive Index, RI, and MultiAngle Light Scattering, MALS, detectors and it was experienced that good separations were obtained with a minimum of time for method development.

In addition, the report covers A4F experiments on Fc-coupled protein for qualification of an SE-HPLC method. In a different experiment Fc-coupled protein were analyzed for possible aggregation under acidic pH conditions. Also experiments with a pegylated protein are described as well as a comparison of large range separation on a long and a short channel design.

Table 1. *Optimized antibody mixture separation scheme.*

Flowrate: 1 ml/min **Channel:** Long **Spacer:** 350M

Step	delta t	Time	Mode	X start	X end	Focus Flow
1	3.00	3.00	Elu	5.00	5.00	-
2	2.00	5.00	Focus	-	-	2.00
3	3.00	8.00	Foc+Inj	-	-	2.00
4	2.00	10.00	Focus	-	-	2.00
5	30.00	40.00	Elu	5.00	1.30	-
6	10.00	50.00	Elu+Inj	0.00	0.00	-

Table 2. *Optimized antibody mixture separation scheme for* sequential *runs.*

Flowrate: 1 ml/min **Channel:** Long **Spacer:** 350M

Step	delta t	Time	Mode	X start	X end	Focus Flow
1	*8.00*	8.00	Elu	5.00	5.00	-
2	2.00	10.00	Focus	-	-	2.00
3	3.00	13.00	Foc+Inj	-	-	2.00
4	2.00	15.00	Focus	-	-	2.00
5	30.00	45.00	Elu	5.00	1.30	-
6	10.00	55.00	Elu+Inj	0.00	0.00	-

Table of Contents

1. Introduction

1.1. Background

The American Food and Drug Administration, FDA, has shown a rising interest in studying product aggregates in therapeutic protein drugs. As reported by FDA's Amy Rosenberg (2006) the formation of large aggregates has been shown to increase the potential immunogenicity of a drug compound. Highly repeated surface elements, such as might be found in large aggregate species, may efficiently induce antibody responses even in the absence of T-cell help. Many therapeutic drugs mimic the structure and function of native proteins. A worst case scenario would be to elicit an antibody response that both targets the administered drug and also induce a response against the body-own protein mimicked.

Although the greatest threat is that of large aggregates these are very hard to detect and quantify in an efficient manner. Therefore the amount of smaller aggregate species such as dimers and trimers are usually analyzed since they are thought to give an indication of the prevalence of large aggregate complexes.

The standard technique for aggregate analyses today is Size-Exclusion High Performance Liquid Chromatography, SE-HPLC. However, when setting up a method for routine use the results need to be compared with results obtained using orthogonal techniques. Orthogonal techniques are techniques that measure the same parameter of interest although the fundamental separation mechanisms are different. Today Sedimentation Velocity Analytical Ultracentrifugation, SV-AUC, is the technique most widely used to validate SE-HPLC methods. However, SV-AUC is a very expensive procedure demanding a high level of expertise. With a price tag of around 15 000 to 30 000 SEK per sample the pressure to find alternative techniques is mounting.

One such alternative technique is Asymmetrical Flow Field-Flow Fractionation, A4F. The technique has been around for over a decade (Wahlund & Giddings, 1987) but has only recently become commercially available. Because of this there is limited literature and experience with A4F available. This study has been performed in order to investigate the capabilities and potential of the technique and to raise the awareness of the possibilities it offer for the Biovitrum Analytical Sciences department.

1.2. Research Topic and Aim

Asymmetrical Flow Field-Flow Fractionation, A4F, is a relatively novel tool for the wider biotech research community. This study will characterize key parameters of A4F. It will also compare separation results obtained with A4F to results obtained with similar, but orthogonal, techniques. Finally, this study will develop an optimized method to separate a given analyte.

1.2.1. Characterization

This study will characterize key parameters of A4F. The focus will be on identifying and describing the key parameters most easily tuned in practical method development. Also the impact of less influential parameters will be described in order to get a wider understanding of different practical aspects in method development.

1.2.2. New Method Development

Throughout this study the main analyte will be a complex mix of IgG antibodies. By using this complex sample one might get a further appreciation of real problems, considerations and trade-offs one has to make when developing a method. The final outcome of this study will be a refined and optimized method of separating monomers, dimers and low molecular weight impurities in a complex antibody sample.

1.2.3. Correlation Studies

For protein characterization, such as identity evaluation in terms of molar masses and sizes, and evaluation of method performance characteristics, mainly in terms of accuracy and selectivity, it is of importance to correlate a technique with orthogonal techniques. This study compares quantitative results obtained from A4F with the orthogonal techniques native PolyAcrylamide Gel-Electrophoresis (native PAGE), Dynamic Light Scattering (DLS), Size-Exclusion High Performance Liquid Chromatography (SE-HPLC) and Sedimentation Velocity Analytical Ultracentrifugation (SV-AUC). Also different qualitative aspects of the techniques will be commented.

1.3. Principles of Techniques

This section will cover the mechanisms of FFF and the special case A4F more in-depth, while only briefly describe the workings of the other techniques that are not explicitly in focus in this report.

1.3.1. Field Flow Fractionation (FFF)

FFF is a family name for several different subtechniques, all based on the same main principle; a physical field is applied perpendicular to a matrix free separation channel, differentially pushing the sample into different flow laminae depending on its hydrodynamic radius (Wahlund & Giddings, 1987), see Figure 1. The name of the specific subtechnique depends on which type of physical field that is exerted: in thermal FFF a temperature gradient is used, in sedimentation FFF a centrifugation field, in electrical FFF an electrical field, and in flow FFF a cross-flow creates the field (Fraunhofer & Winter, 2004).

FFF separation takes place in a flat, thin, rectangular-shaped channel. As opposed to many other chromatographic and electrophoretic techniques, there is no gel matrix involved. Carrier liquid is introduced in one end of the channel and exits at the other end. Because of friction against the walls, the carrier liquid moves faster in the middle of the channel, this creates a parabolic flow profile. The sample is introduced near to the inlet end of the channel. A perpendicular force-field applied to the channel pushes the sample components towards one wall of the channel, the accumulation wall.

There are two modes of elution, normal and steric. In this study only normal mode was used. Here, because of diffusion the sample components will not lie flat against the accumulation wall all the time. The mean distance of components depends on the diffusion coefficient of the component. Smaller molecules, with a smaller hydrodynamic radius, have a larger diffusion coefficient and will therefore be statistically further away from the accumulation wall. This means that smaller molecules will spend more time in a faster flow, and therefore elute prior to larger molecules. This is the basis of the separation. In steric mode, buoyancy effects of very large molecules will instead place them closer to the middle of the channel flow and therefore they will elute first.

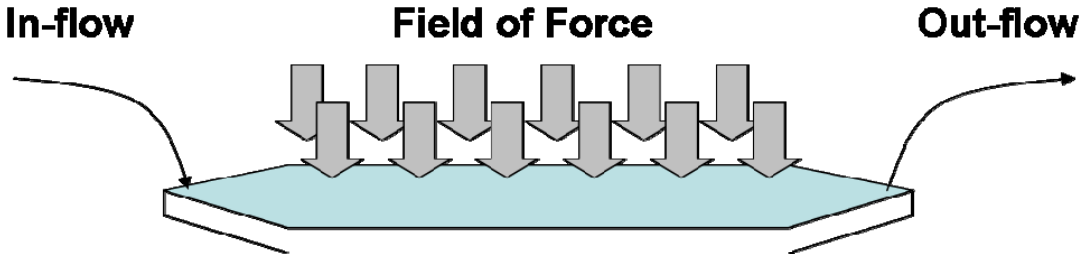

Figure 1. *In FFF a physical field is applied perpendicular to a matrix free separation channel, differentially pushing the sample into different flow laminae depending on its hydrodynamic radius.*

1.3.2. Asymmetrical Flow Field-Flow Fractionation (A4F)

A4F is a sub-technique of FFF. Here the field is created by a crossflow through the accumulation wall. To prevent sample loss the accumulation wall consists of an exchangeable ultra-filtration membrane supported by a porous metal frit.

Originally, flow FFF created a crossflow by pumping liquid through the upper wall that also was porous. What makes A4F asymmetric is that the actual crossflow is split off the carrier liquid introduced at the inlet end of the channel (Wahlund & Giddings, 1987). The introduction of the total amount of liquid used at one end of the channel and the subsequent loss of liquid through crossflow lead to differences in the flow velocity through the channel. To counter-act these differences a trapezoidal channel geometry is used where the channel becomes narrower towards the end to retain the flow velocity.

The design with one permeable wall permits focusing of the samples prior to the elution step. In this focusing step the flow from the outlet end of the channel is reversed. Carrier liquid now enters the channel both from the inlet and the outlet end, and exits through the bottom membrane. By adjusting the ratio between the inflows the boundary line where the two flows meet is also adjusted. This narrow line is where an injected sample will focus, so typically the flow rates are adjusted to focus the sample in the beginning of the channel close to the sample injection point.

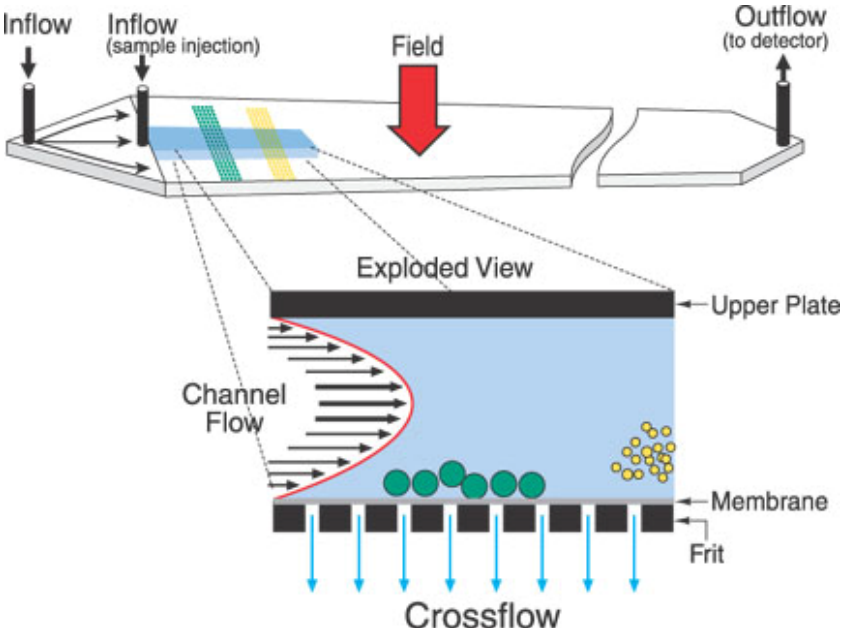

Figure 2. *Schematic figure of an A4F channel during elution. The narrow bands of the sample components have begun to separate because of different mean distribution height in the channel, due to different diffusion coefficients. The crossflow is split off the channel inflow. The sample is with a thin ultra-filtration membrane prevented from exiting the channel with the crossflow. Please note that the sample injection port is not open during the elution step. (Illustration used with permission from Wyatt Technology, Santa Barbara, CA)*

1.3.3. Dynamic Light Scattering (DLS)

In DLS fluctuations in the intensity of light scattered from a protein solution is studied over timescales from 0.1 µs to 0.1 s. When radiating molecules in solution with light, laser in this case, they scatter light. Different types of molecules scatter different amounts of light, and larger molecules scatter more than smaller. It is also so that macromolecules in solution move in a random manner, so called Brownian motion. This movement gives rise to fluctuations in the intensity of the scattered light. Larger molecules move more slowly than smaller ones, therefore the time scale of the scattering fluctuations provides a measure of molecular size. (Arakawa *et al*, 2007)

1.3.4. Native Polyacrylamide Gel-Electrophoresis (Native PAGE)

Native PAGE separates proteins in a polyacrylamide gel matrix in a native manner, without SDS or reducing agent. Contrary to SDS-PAGE, the proteins are neither linearized nor reduced. By running the samples in a native, non-denatured state it is possible to preserve and separate aggregated proteins and protein complexes. All the proteins in the sample analyzed carry their native charge at the pH of the gel, therefore proteins separate both according to their different electrophoretic mobilities and the sieving effects of the gel. (Walker, 2005)

1.3.5. Sedimentation Velocity Analytical Ultracentrifugation (SV-AUC)

In SV-AUC a protein sample is subjected to a high centrifugal force, up to 250 000*g*, which is counteracted by buoyancy and frictional force. The combination of the three forces results in a constant velocity of the macromolecule towards the bottom of the cell. During the experiment

the distribution of macromolecules along the radial axis is periodically measured. The experiment is usually run until all the proteins have sedimented to the bottom. Subjecting the data collected to different analyses give a distribution of the sedimentation coefficients measured. The output resembles a chromatogram where each peak corresponds to a different species and the area under each peak is proportional to the concentration. (Markova, 2007)

1.3.6. Size-Exclusion High Performance Liquid Chromatography (SE-HPLC)

SE-HPLC uses porous particles to separate molecules of different sizes. These particles are packed in a column on which a flow is applied. Proteins and their aggregated complexes are separated because they penetrate, by diffusion, into the stationary porous particles to different extents. Larger molecules, such as aggregates, permeate the stationary phase less or not at all and therefore elute early, while small molecules with greater access to the porous particles elute more slowly (Gabrielson *et al*, 2007)

2. Materials and Methods

2.1 Analytes

2.1.1 Antibody Mixture, AbM

The main analyte in this project consists of a mix of 25 different human immunogamma globulins, IgGs. The original sample used was a Working Standard, WS, without any significant contaminations of other proteins. The sample concentration was 0.73 mg/ml.

Aggregates, mainly different IgG dimer species, were induced by UV radiation (UV-irradiator TL-900, Camag) of the WS. Aggregate levels of approximately 20 % was obtained. The aggregate preparation was dispensed in 100 µl aliquots and stored in -70 °C until use.

2.1.2. BioRad Gel Filtration Standard

The gel filtration standard is a mixture of five molecular weight markers, with molecular masses ranging from 1.35 to 670 kD. It is a calibration standard for size exclusion columns used in protein purification. The included proteins are: vitamin B12, 1.35 kDa; equine myoglobin, 17 kDa; chicken ovalbumin, 44 kDa; bovine gamma globulin, 158 kDa; and thyroglobulin, 670 kDa.

2.1.4. Fc-Coupled Protein

The Fc-coupled protein is a fusion protein where two IgG Fc-parts have been fused to a therapeutic protein. The resulting protein weights about 110 kDa.

2.1.5. HMW Calibration Kit

Like the BioRad GF Standard also the HMW calibration kit from General Electric Healthcare consists of five different proteins. This kit focus on slightly higher molecular weight proteins though. The proteins are albumin, 66 kDa; lactate hydrogenase, 140 kDa; catalase, 232 kDa; ferritin, 440 kDa; and thyroglobulin, here 669 kDa.

2.1.6. Pegylated Protein

In the Additional experiments section a small pegylated protein was analyzed. The protein with the attached polyethylene glycol tail weights around 40 kDa.

2.2. Design of Experiments

In order to characterize different A4F parameters the experimental framework Design of Experiments, DoE, was used. This section draws heavily on information found in Design of Experiments: Principles and Applications by Eriksson *et al* (2000).

Intuitively, the way of characterizing several different parameters are to vary them one at a time until you find an optimal setting for each parameter. However, if there are interactions between factors one is likely to get stuck at a point which is not the optimum. Changing one factor at the time (COST) also gives different implications with different starting points, see Figure 3. This intuitive approach both requires plenty of experiments and is not very correct.

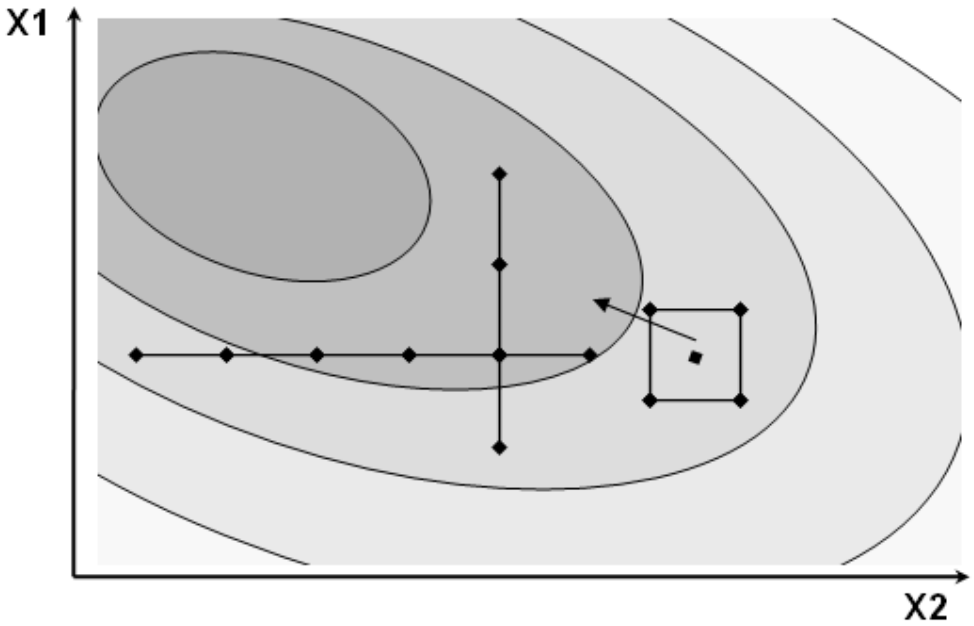

Figure 3. *The COST approach and the DoE approach. Changing all parameters at once with a DoE experimental design is likely to give better information on where the optimum is located.*

A better way of characterizing multiple parameters is to create a selected *set* of experiments, in which *all* the chosen parameters are varied simultaneously. From the set of experiments a statistical model is generated. This model both helps to find the optimal point for your problem and also gives information on how important different parameters are and possible correlation effects between parameters.

The way the parameters are varied is not contingent upon the result of the last performed experiment; rather the parameters are varied according to a predetermined experimental design. This design typically centers around a given point, and for *n* parameters the experimental region is determined by an *n*-dimensional box. In a full factorial design the individual experiments are set to investigate each corner of this box and its centerpoint, see Figure 4 a).

If the number of parameters is very large it might not be practical to carry out a full fractional design. With a fractional factorial design you might get sufficient information with a highly reduced number of experiments, see Figure 4 b). In other cases you might not get enough information from a plain full fractional design. This is especially the case when you have curvature in your responses. With only corner experiments you can only model linear responses correctly. To model curvature you also need to add axial experimental points, see Figure 4 c).

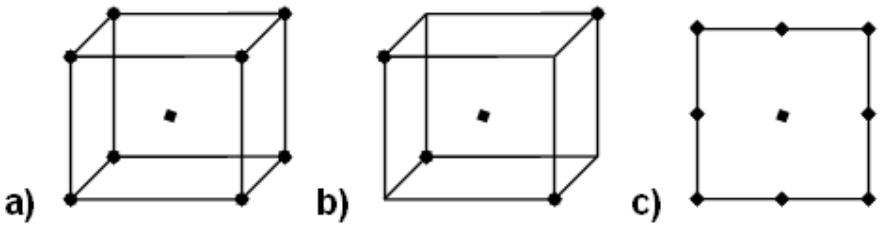

Figur 4. a) *A three parameter full factorial experimental design.* ***b)*** *Example of a three parameter fractional factorial design.* ***c)*** *A two parameter full factorial design complemeted with axial points to detect curvature.*

The DoE investigations were supported by the software Modde 8.0 from Umetrics. Modde was used both for the design of the experiment matrix and for the subsequent evaluation of the results. Two experimental sets were performed: first a screening and then an optimization set.

2.2.1. Screening

In a screening trial the objective is to identify critical parameters and to get a rough estimate of how these affects the measured response. For an overview of the conducted experiments see Table 3.

Table 3. *Experiments conducted in the Screening design. Experiment numbers 17 to 20 are center point runs.*

Exp No	Run Order	Membrane	Spacer height [µm]	Channel width [mm]	Crossflow [ml/min]	Crossflow gradient	Channel flow [ml/min]	Sample load [µl]	Focus time [min]	$Block	Subjective Separation Score
1	16	Cellulosa	250	10	0,5	0	0,5	5	2	-1	
2	3	Polyetersulfon	250	10	0,5	0	1,5	25	4	-1	
3	19	Cellulosa	490	10	0,5	1	0,5	25	4	-1	
4	1	Polyetersulfon	490	10	0,5	1	1,5	5	2	-1	
5	11	Cellulosa	250	20	0,5	1	1,5	25	2	-1	
6	7	Polyetersulfon	250	20	0,5	1	0,5	5	4	-1	
7	17	Cellulosa	490	20	0,5	0	1,5	5	4	-1	
8	10	Polyetersulfon	490	20	0,5	0	0,5	25	2	-1	
9	15	Cellulosa	250	10	2	1	1,5	5	4	-1	
10	4	Polyetersulfon	250	10	2	1	0,5	25	2	-1	
11	20	Cellulosa	490	10	2	0	1,5	25	2	-1	
12	2	Polyetersulfon	490	10	2	0	0,5	5	4	-1	
13	12	Cellulosa	250	20	2	0	0,5	25	4	-1	
14	8	Polyetersulfon	250	20	2	0	1,5	5	2	-1	
15	18	Cellulosa	490	20	2	1	0,5	5	2	-1	
16	9	Polyetersulfon	490	20	2	1	1,5	25	4	-1	
17	14	Cellulosa	350	15	1,25	0,5	1	15	3	-1	
18	13	Cellulosa	350	15	1,25	0,5	1	15	3	-1	
19	5	Polyetersulfon	350	15	1,25	0,5	1	15	3	-1	
20	6	Polyetersulfon	350	15	1,25	0,5	1	15	3	-1	

2.2.1.1 Experimental Design Specifics

The design used was a fractional factorial design with resolution IV, 2^{8-4}. This design requires 16 experiments plus center points. Four center point experiments were conducted, bringing the total number of experiments to 20. The four center points were divided between each of the two qualitative settings for the membrane type.

2.2.1.2 Description of Screening Factors

Eight factors were identified as being of interest for a screening purpose.

1) Different types of membranes have different permeability and possibly different interaction with the sample components. The channel membrane was either regenerated Cellulose (Wyatt Technology, Art.No.: 14705) or Polyethersulphone (Wyatt Technology, Art.No.: 920105), both with a pore size cut-off of 10 kDa. These are the two most commonly used membrane types, and the cut-off were considered to be in a size that was practical both in this study but also in most other standard runs on proteins.

2) The spacer height greatly affects the flux as well as the flow profile in the channel. Three heights of spacers were considered: 490, 350, and 250 μm. These are the three thickest spacers supplied in the Eclipse F set of spacers (Wyatt Technology Europe, Art.No.: 380). Thicker spacers give a higher retention time but also the opportunity to load more sample on the channel before it gets overloaded.

3) Also the channel width greatly affects the flux. However, here the correlation is slightly more complicated, since a wider channel has a larger surface and therefore distributes the crossflow force over a larger area. In literature (Wahlund and Giddings, 1987) it has been shown that for a trapezoidal channel, as the ones we use, it is theoretically the ratio between the width of the inlet end and the width of the outlet end that determines the impact from the channel area geometry on the separation time. For the Eclipse F set of spacers though, the inlet to outlet width ratio is fairly constant which reduces the width-factor to a way to regulate the sample concentration. A wider channel can have a correspondingly higher sample load than a more narrow channel but still retain the same sample concentration distribution. Three different inlet widths are available and were used. See Table 4.

Table 4. *Inlet and outlet widths of the spacers in Eclipse F set of spacers.*

Inlet width [mm]	Outlet width [mm]	Inlet / Outlet
21,5	6	3,583
16,5	4	4,125
11,5	3	3,833

4) The crossflow, 5) the crossflow gradient and 6) the channel flow are all parameters that are easy to control and that may have a large impact on the separation. For the purpose of this screening a center point elution scheme was developed. This scheme was developed to give a reasonable separation and was used as a base around which the screening parameters were varied. See Table 5 below. A Crossflow Gradient of 1 here means that after 30 minutes, i.e. at the end of a run, the Crossflow had linearly dropped to 0 ml/min from its initial value. A gradient of 0,5 mean that the crossflow linearly drops to half its initial value, and the setting 0 means that there was no gradient at all.

Table 5. *Flow settings for the screening experimental design.*

	High	Center	Low
Channel flow [ml/min]	1,5	1	0,5
Crossflow [ml/min]	2	1,25	0,5
Crossflow Gradient	1	0,5	0

The seventh factor to be employed was 7) sample load. This was set to either 5 µg or 25 µg, with a center point value of 15 µg. A high sample load to gives a good signal, but a too high load might affect the peak symmetry and other aspects of the separation.

Finally, 8) the focus time was investigated. To get narrow peaks it is important to give the sample long enough time to focus into a thin line. However, if a very high sample concentration is achieved during the focus step this might promote the association into aggregates of the sample. This is of course very serious, especially when the amount of aggregate in the original, native sample is studied. The sample injection focus time was set to maximum 4 minutes and minimum 2 minutes, with a center point at 3 min.

2.2.1.3 Responses

No baseline separation was achieved, therefore strict measures applying to a two peak separation were difficult to achieve. To classify the grade of separation a response termed subjective separation score was implemented. Here the runs were given a score of 1 (bad) -10 (excellent) based on the over-all separation profile. Attention was given mainly to amount of peak separation but also to the symmetry of the peaks. Moreover, responses such as peak symmetry and relative retention were applied based solely on the main peak.

2.2.1.4 Complementary Experiments

While the responses showed signs of great curvature, a set of complementary experiments were added to the experimental design. These experiments were designed as axial points to be able to estimate the influence of curvature from certain parameters. The parameters chosen to be investigated further were channel flow, crossflow, crossflow gradient and channel width. For each of the four factors two new experiments were added and an additional two centerpoints were also added, see Table 6. In the evaluation of the complemented design a block factor was also added. This is to compensate for any changes in the instrumentation properties between the original screening set and the set of complementary experiments.

Table 6*. Complementary Experiments.*

Exp No	Run Order	Membrane	Spacer height [µm]	Channel width [mm]	Crossflow [ml/min]	Crossflow gradient	Channel flow [ml/min]	Sample load [µl]	Focus time [min]	$Block	Subjective Separation Score
21	26	Cellulosa	350	10	1,25	0,5	1	15	3	1	
22	30	Polyetersulfon	350	20	1,25	0,5	1	15	3	1	
23	22	Cellulosa	350	15	0,5	0,5	1	15	3	1	
24	27	Polyetersulfon	350	15	2	0,5	1	15	3	1	
25	21	Cellulosa	350	15	1,25	0	1	15	3	1	
26	29	Polyetersulfon	350	15	1,25	1	1	15	3	1	
27	24	Cellulosa	350	15	1,25	0,5	0,5	15	3	1	
28	28	Polyetersulfon	350	15	1,25	0,5	1,5	15	3	1	
29	23	Cellulosa	350	15	1,25	0,5	1	15	3	1	
30	25	Cellulosa	350	15	1,25	0,5	1	15	3	1	

2.2.1.5 Comment on the Run Order

In the fractional factorial design that was chosen, and as in all designs, the run order of the experiments should be randomized. This is to minimize the risk of trends in the data due to any type of drift in the system over time. Also here the run order was originally randomized. However, due to practical consideration the run order was subsequently customized.

The underlying reason for this is of practical nature. To change a membrane or the spacer in A4F is very time consuming. The channel has to be disconnected, disassembled, cleaned, reassembled, reconnected, and the membrane has to be flushed and reconditioned. All in all

this entire procedure takes a little bit over two hours. To reduce this experimental down time experiments using the same membrane and spacer were grouped together. A new run order was constructed where the lowest original run order number was used to determine the order of the pair of experiments sharing the same membrane and spacer. In an effort to further minimize the down time the runs were also grouped in a similar manner according to which membrane they were using.

The run order of the complementary runs that were added was customized in the same way.

2.2.2. Optimization

In the screening experiment the most important factors were identified by varying the parameters quite significantly. In the optimization experiment the purpose was to vary the most important factors over a narrower range, starting with an already fairly good separation.

2.2.2.1 Experimental Design Specifics

With a so called central composite experimental design it is possible to model five factors, with curvature, in 26 experiments plus center points. In this experiment six center points were used, bringing the total number of experiments to 32. The center points were also used as System Suitability Tests; therefore the run order for them was customized to spread them out as much as possible. This is likely to rather exaggerate than hide replicate errors. For an overview of the conducted experiments see Table 7.

Table 7. *Experimental Design for the optimization runs. The table shows the run order of the experiments, the factors and their settings, and relevant responses used.*

Exp No	Run Order	Channel Flow [ml/min]	Crossflow to Channel Flow	Gradient	Sample Load [µl]	Focus Time [min]	Percentage of Aggregation	Resolution Peak 4-3	deltaRt Peak 4-3 [min]	Retention Time Peak 4 [min]
1	12	0,6	3	0,25	3	4				
2	3	1	3	0,25	3	2				
3	8	0,6	5	0,25	3	2				
4	25	1	5	0,25	3	4				
5	2	0,6	3	0,75	3	2				
6	28	1	3	0,75	3	4				
7	26	0,6	5	0,75	3	4				
8	22	1	5	0,75	3	2				
9	30	0,6	3	0,25	7	2				
10	15	1	3	0,25	7	4				
11	18	0,6	5	0,25	7	4				
12	29	1	5	0,25	7	2				
13	14	0,6	3	0,75	7	4				
14	13	1	3	0,75	7	2				
15	24	0,6	5	0,75	7	2				
16	16	1	5	0,75	7	4				
17	27	0,4	4	0,5	5	3				
18	5	1,2	4	0,5	5	3				
19	20	0,8	2	0,5	5	3				
20	17	0,8	6	0,5	5	3				
21	7	0,8	4	0	5	3				
22	19	0,8	4	1	5	3				
23	23	0,8	4	0,5	1	3				
24	9	0,8	4	0,5	9	3				
25	4	0,8	4	0,5	5	1				
26	31	0,8	4	0,5	5	5				
27	11	0,8	4	0,5	5	3				
28	10	0,8	4	0,5	5	3				
29	6	0,8	4	0,5	5	3				
30	1	0,8	4	0,5	5	3				
31	21	0,8	4	0,5	5	3				
32	32	0,8	4	0,5	5	3				

Five factors were considered to be ideal for this study. An additional factor would have increased the number of experiments needed to 44, whilst a four factor experiment still would have needed 24 experiments, plus center points for both examples. (Eriksson *et al*, 2000)

2.2.2.2 Optimization Factors

The optimization factors were chosen based mainly on the outcome of the screening study, but also with respect to practical matters, theory, and sound judgements acquired from other experiments.

The most important parameters, as they both affect the separation heavily and are flexible and easy to adjust, are the different flow parameters. These basically determine the channel flow, the crossflow and an eventual crossflow gradient. To be in closer accordance with both theory and practical experience, one factor is the ratio of crossflow to channel flow. As a moderator of how high the flows should be another factor was the channel flow. Also the gradient factor was determined to be important enough to optimize.

Sample load and focus time factors were thought to affect the peak width in a separation. Additionally, sample load and focus time were considered important to investigate to see any possible influence on aggregate formation.

By keeping the same membrane and the same spacer it was possible to automate the experiments. This was done by setting up a sequence run where the running parameters were pre-programmed. Thereafter the runs were automatically run in sequence without any further input between each run. A list of the factors and their settings can be seen in Table 8.

Table 8. *The optimization factors and their settings.*

Factors	Low axial point	Ordinary min	Center point	Ordinary max	High axial point
Channel Flow [ml/min]	0.4	0.6	0.8	1.0	1.2
Crossflow to Channel Flow	2	3	4	5	6
Gradient	0	0.25	0.5	0.75	1
Sample Load [ul]	1	3	5	7	9
Focus Time [min]	1	2	3	4	5

2.2.2.3 Responses

The optimization runs generally gave a fairly good separation, although not with baseline separation between the monomer and dimer peak. Because of the limited separation a customized resolution measure was devised. Literature (Agilent Technologies, 2000) gives a resolution measure using the retention times for the different peaks and the width of the peaks at half their maximum height. This measure was used with the modification that for peak 2 and peak 4 the peak widths were estimated to be two times the width of the side possible to calculate, see Figure 5. In addition to the resolution measure, measures of ΔR_t, the difference in retention times, between the various peaks were taken. Also a measure of possible aggregation was introduced by comparing the area percent of the peaks.

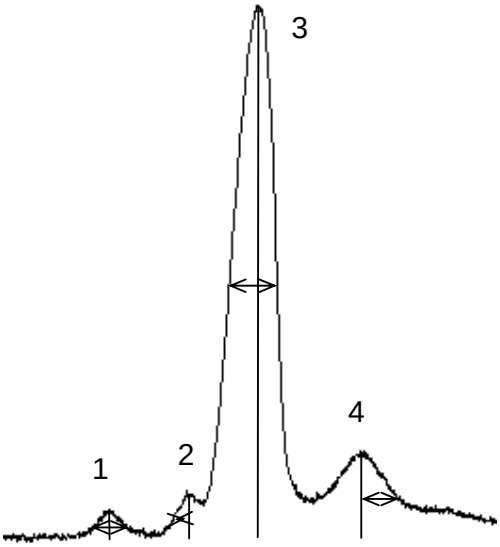

Figure 5. *True half-width was used for peaks 1 and 3, whereas two times the one-sided half-width was used for peaks 2 and 4.*

2.3. Correlation Studies

A correlation study was performed with the intent to both compare the actual results obtained and to describe qualitative characteristics of the different techniques. Direct comparison with the same analyte was carried out between A4F, SE-HPLC, DLS and Native PAGE. A similar study with a different preparation of the analyte was previously carried out by Dr Christine Hägglund and this will be used to cross-correlate results also from analytical ultra-centrifugation.

2.4. Techniques

2.4.1. Asymmetrical Flow Field-Flow Fractionation

The A4F-channel was controlled by an Eclipse 2 system coupled to an Agilent 1100 HPLC system. The Agilent system consisted of a G1379A degasser, a G1311A quaternary pump, a G1367A autosampler temperated by a G1330B autosampler thermostat. The Eclipse 2 system was built for aqueous (non-organic) solutions and had a SE-HPLC switcher valve. The valve controlled whether an A4F channel or a column should be used for separation. Although not used here, a column separation could be temperature controlled by a G1316A column compartment.

Two different A4F channels were employed, unless otherwise stated the long aqueous channel was the one used in all measurements. The short aqueous channel was only used in experiments to compare the two channels. All spacers used were trapezoidal; for the long channel, spacers were taken from the Eclipse F set of spacers (Wyatt Technology). The spacers used were either 480 µm, 350 µm or 250 µm high and had a maximum width of 21.5 mm, 16.5 mm or 11.5 mm. All spacers for the long channel were 240 mm long. The spacer used in the short channel was 152 mm long, had 16.5 mm maximum width and was 350 µm high. Two different membranes were used: regenerated cellulose or polyethersulphone, both

with a 10 kDa nominal cut off. Unless otherwise stated in the experiments the regenerated cellulose membrane was used. Also, unless otherwise stated the mobile phase used consisted of Dulbecco´s Phosphate Buffered Saline (D-PBS) without calcium or magnesium, pH 7.4, from Invitrogen.

The A4F system was equipped with three different detectors: UV, MALS and RI. The UV-detector was a Agilent G1314A variable wavelength detector controlled by Agilent Chemstation and set at either 214 nm or 280 nm. Multiangle light scattering was measured at three different angles by a Wyatt Technology miniDAWN. Refractive index was measured by an Optilab rEX, also from Wyatt Technology. Both the MALS and the RI detector measured at 690 nm wavelength and were controlled by the software ASTRA V (version 5.3.2.13, Wyatt Technology). ASTRA was also used for data collection, processing and evaluation for all the detectors.

2.4.2. Dynamic Light Scattering

Dynamic Light Scattering experiments were conducted on a DynaPro Titan from Wyatt Technologies equipped with a DynaPro Plate Reader from the same company. The software used for capturing, processing and evaluation of the data was Dynamics V6 (Wyatt Technologies). Data was collected in ten 10 second intervals and an autocorrelation function was established. Calculations of R were made assuming the spherical form of light scattering particles (i.e. Rh = effective hydrodynamic radius) in PBS buffer. Viscosity = 1.019 cp at 20 °C was automatically corrected for the temperature of the measurements: 25 °C.

2.4.3. Native Polyacrylamide Gel Electrophoresis

Native PAGE was run with antibody mixture samples, both the WS and the aggregated sample. Also HMW calibration kit from General Electric Healthcare was run as a molecular weight standard.

The gel used was a 4-20% gradient Novex Tris-Glycine gel, 1 mm thick with 10 wells. The running buffer was Novex TrisGlycine Running Buffer and the sample buffer was Native LDS Sample Buffer. The gel was placed in a XCell Mini-Cell system. This was connected to an Electrophoresis Power Supply (Amersham Biosciences EPS 601) which was set on 65V, 5mA, 40W and running time 20 hours.

After the run the gel was washed and placed five hours in fixation buffer (10% Ethanol, 7% Acetic Acid). It was thereafter stained over night in Sypro Ruby Protein Gel Stain (BioRad) for 18 hours. Next, it was destained for 30 min in Destaining Buffer (10% Ethanol, 7% Acetic Acid, same as fixation buffer) and washed. Finally the gel was scanned and developed in the digital imaging system ProXpress 2D (Perkin Elmer). The resulting digital image was then evaluated using ImageMaster 1D Gel Analysis (Amersham Pharmacia).

2.4.4. Sedimentation Velocity Analytical Ultracentrifugation

SV-AUC analysis was performed by the company iNovacia AB in Stockholm. AUC scans were carried out on ProteomeLab Optima XI instrument from Beckman Coulter. The readout from interference optics was recorded in the cause of 5 h at 50 krpm and 20ºC. Four samples were run, three different AbM samples with varying degrees of aggregates as well as a reference sample with the same buffer but without proteins.

2.4.5. Size-Exclusion High Performance Liquid Chromatography

Size-Exclusion High Performance Liquid Chromatography, SE-HPLC, was run on an Agilent 1100 HPLC system. This was equipped with a G1322A degasser, a G1312A binary pump, a G1329 autosampler thermically controlled by a G1330 thermostat, a G1316A column compartment, and a G1315B diode array detector. The column was a TSK G4000SW 7.5/60 from TOSOH BIOSCIENCE. The autosampler temperature 4 ± 3 °C and the detection wavelength was 214 nm. The mobile phase was a 0.2 mol/L sodium phosphate buffer, pH 6.5, with 0.15 mol/L NaCl and 10% EtOH. The flowrate was 1.0 ml/min. For data acquisition, integration and report generation the software Chemstation Plus from Agilent was used.

3. Results and Discussion

In this section the results will be presented and commented. The structure follows the topics and aims of the study. First results corresponding to the characterization of the system will be presented. This mainly entails experience gathered through a screening and an optimization design of experiments trial. After the characterization A4F results will be correlated to other techniques. Thereafter the development of a new method will be discussed before, lastly, the presentation of some additional sample runs that have been conducted in this study.

3.1. Characterization

Results concerning the characterization of the A4F system will be presented. To identify and describe the influence of different parameters the Design of Experiments (DoE) framework has been used on a real separation problem. A first screening trial identifies key parameters. These key parameters are then used to optimize a separation.

3.1.1. DoE - Screening

A model was developed based on a point system of the subjective separation score. This subjective scoring was based on a visual appreciation of the grade of separation as well as the symmetry of the peaks. The model achieved from the initial fractional factorial design showed a strong influence of curvature on the response. This meant that one or more of the factors did not affect the response in a linear manner. To be able to model the curvature correctly the design was complemented with additional experiments. All experiments and their response can be seen in Table 9 below.

***Table 9**. Screening experimental set. Experiments 1-20 from original design, number 21-30 are complementary experiments to be able to model curvature.*

Exp No	Exp Name	Run Order	Incl/Excl	Membrane	Spacer height [µm]	Channel width [mm]	Crossflow [ml/min]	Crossflow gradient	Channel flow [ml/min]	Sample load [µl]	Focus time [min]	$Block	Subjective Separation Score
1	N1	16	Incl	Cellulosa	250	10	0,5	0	0,5	5	2	-1	4
2	N2	3	Incl	Polyetersulfon	250	10	0,5	0	1,5	25	4	-1	1
3	N3	19	Incl	Cellulosa	490	10	0,5	1	0,5	25	4	-1	5
4	N4	1	Incl	Polyetersulfon	490	10	0,5	1	1,5	5	2	-1	2
5	N5	11	Incl	Cellulosa	250	20	0,5	1	1,5	25	2	-1	2
6	N6	7	Excl	Polyetersulfon	250	20	0,5	1	0,5	5	4	-1	1
7	N7	17	Incl	Cellulosa	490	20	0,5	0	1,5	5	4	-1	3
8	N8	10	Incl	Polyetersulfon	490	20	0,5	0	0,5	25	2	-1	3
9	N9	15	Incl	Cellulosa	250	10	2	1	1,5	5	4	-1	7
10	N10	4	Incl	Polyetersulfon	250	10	2	1	0,5	25	2	-1	4
11	N11	20	Incl	Cellulosa	490	10	2	0	1,5	25	2	-1	3
12	N12	2	Incl	Polyetersulfon	490	10	2	0	0,5	5	4	-1	3
13	N13	12	Incl	Cellulosa	250	20	2	0	0,5	25	4	-1	4
14	N14	8	Incl	Polyetersulfon	250	20	2	0	1,5	5	2	-1	3
15	N15	18	Incl	Cellulosa	490	20	2	1	0,5	5	2	-1	6
16	N16	9	Incl	Polyetersulfon	490	20	2	1	1,5	25	4	-1	6
17	N17	14	Incl	Cellulosa	350	15	1,25	0,5	1	15	3	-1	7
18	N18	13	Incl	Cellulosa	350	15	1,25	0,5	1	15	3	-1	7
19	N19	5	Incl	Polyetersulfon	350	15	1,25	0,5	1	15	3	-1	7
20	N20	6	Incl	Polyetersulfon	350	15	1,25	0,5	1	15	3	-1	7
21	C21	26	Incl	Cellulosa	350	10	1,25	0,5	1	15	3	1	6
22	C22	30	Incl	Polyetersulfon	350	20	1,25	0,5	1	15	3	1	2
23	C23	22	Incl	Cellulosa	350	15	0,5	0,5	1	15	3	1	1
24	C24	27	Incl	Polyetersulfon	350	15	2	0,5	1	15	3	1	4
25	C25	21	Incl	Cellulosa	350	15	1,25	0	1	15	3	1	4
26	C26	29	Incl	Polyetersulfon	350	15	1,25	1	1	15	3	1	2
27	C27	24	Incl	Cellulosa	350	15	1,25	0,5	0,5	15	3	1	5
28	C28	28	Incl	Polyetersulfon	350	15	1,25	0,5	1,5	15	3	1	3
29	C29	23	Incl	Cellulosa	350	15	1,25	0,5	1	15	3	1	4
30	C30	25	Incl	Cellulosa	350	15	1,25	0,5	1	15	3	1	4

To get a better overview of the responses a replicate plot was studied, see Figure 6. Here can be seen that the score of the replicated center points (17 and 18; 19 and 20; and 29 and 30) are generally higher than the other responses. This is a clear sign of curvature in the model. It also

means that the original setting around which the experiment was centered gave a comparatively good separation.

Another thing that can be seen in the replicate plot is that the score for the center points in the original design is much higher than the center point score in the complementary design, even though they have the same experimental settings. This difference reflects an external change to the system between the original and the complementary experiment set.

The actual change that took place was that a faulty setting was detected. The setting regulated the distribution between the channel and the crossflow. In the original experiments the separation had taken place during actual conditions that differed from those that were reported and were specified in the settings. To try to compensate for this a factor was introduced to model system change, the block factor. However, the spread between the individual center point pairs is non-existent, indicating an otherwise robust system.

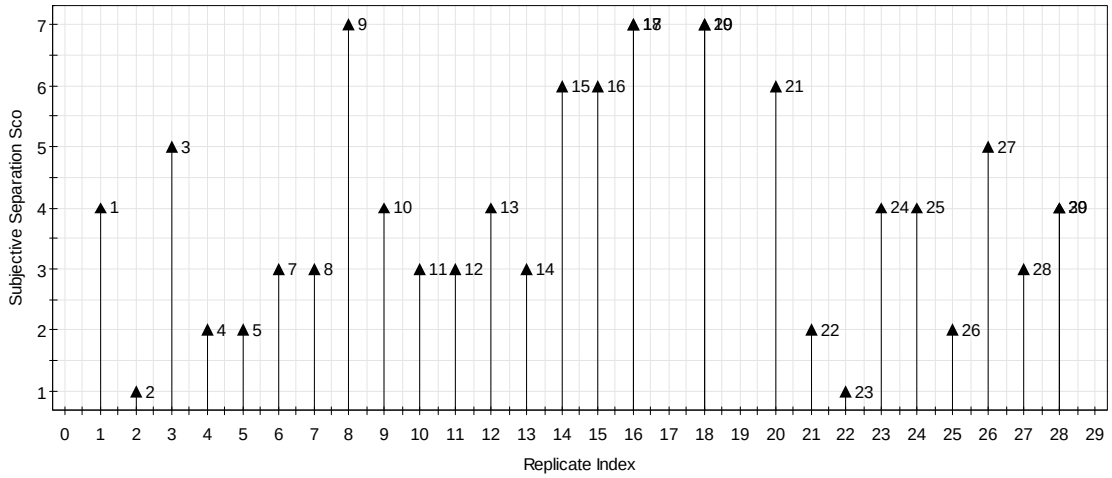

Figure 6. *Replicate plot for the subjective separation score response of the screening experiment. Bars are labelled with experiment number. Replicated center points are modelled in the same bars. The big difference between the original (17-20) and the complementary (29-30) center points indicates a significant system change.*

When constructing the model an outlier was identified using a normal probability plot of residuals, see Figure 7. This outlier was deleted and was not incorporated in neither the model nor the replicate plot above. The reason for the behaviour of the outlier could be that it was run during extremely low flow rates that might have disturbed the stated channel flow to cross flow ratio.

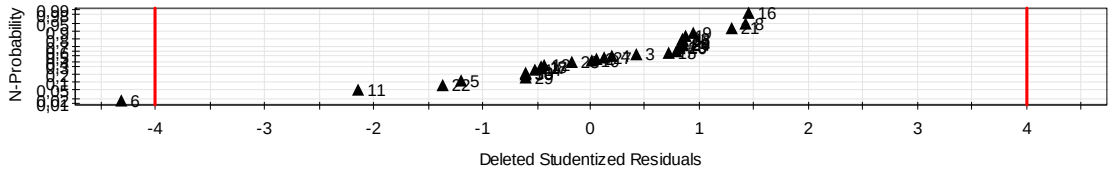

Figure 7. *Experiment 6 was detected as an outlier with this normal probability plot of the residuals. Dots are labelled with experiment numbers. N=30, DF=17, R2=0.797 and Q2=0.128.*

The model was fitted using multiple linear regression (MLR) using 29 samples. The regression coefficients are shown, with a 95% confidence level, in Figure 8. However, considering the R^2/Q^2 values the model suggested was deemed **not valid**. The R^2 value is fairly high, 0.898, but the Q^2 value is comparatively low, 0.597. The Q^2 value in itself is not unacceptably low for a screening trial, but for the model to be valid the difference between R^2 and Q2 shouldn't be greater than 0.2-0.3 (Eriksson *et al*, 2000).

The block factor regression coefficient is the second biggest, showing the big impact of the system change between the runs. A problem with the model is that the greater part of the experiments were carried out before the system change, with settings that don't reflect the actual flow distribution as reported after the change.

However, even though the predictive power of the model is limited it still gives a hint of which factors are the most important. This information was together with literature much influential when choosing the factors to be investigated in the optimization trial.

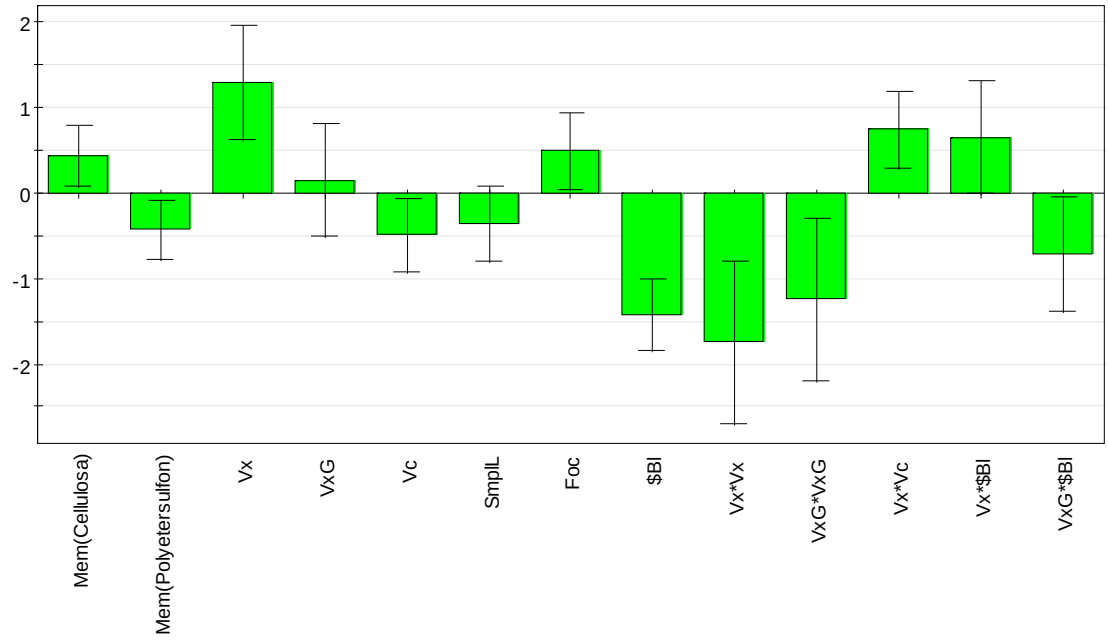

Figure 8. *The coefficient plot for the subjective separation score response of the screening model. The error bars represent a 95 % confidence level. Note the strong curvature (Vx*Vx) and the influence of the block factor $Bl. The crossflow gradient factor VxG is kept even though the error bar overlap zero, this is to preserve other terms where it is incorporated (VxG*VxG and VxG*$Bl). N=29, DF=16, R2=0.898 and Q2=0.597.*

3.1.2. DoE – Optimization

In the experimental design for the optimization trial five factors were evaluated and four responses measured, see Table 10. There were four discernable peaks in the runs. For experiments number 1, 5, 9, 13, 17 and 19 peak three and four could not be separated. The measurements for these runs have therefore been removed from the responses Aggregate percent and Resolution peak 4-3 since a lack of separation between the peaks could disturb the results. For experiment 17 the retention time for peak 4 was removed as an outlier, this is discussed below.

Table 10. *Optimization experimental set. Experiments 17-26 are axial points, 27-32 are center points.*

Exp No	Run Order	Channel Flow [ml/min]	Crossflow to Channel Flow	Gradient	Sample Load [µl]	Focus Time [min]	Percentage of Aggregation	Resolution Peak 4-3	deltaRt Peak 4-3 [min]	Retention Time Peak 4 [min]
1	12	0,6	3	0,25	3	4			2,42	9,62
2	3	1	3	0,25	3	2	0,207	2,79	2,57	10,25
3	8	0,6	5	0,25	3	2	0,208	2,76	3,45	14,05
4	25	1	5	0,25	3	4	0,189	2,23	3,56	15,37
5	2	0,6	3	0,75	3	2			2,06	8,9
6	28	1	3	0,75	3	4	0,229	2,69	2,22	9,48
7	26	0,6	5	0,75	3	4	0,227	2,73	2,79	12,44
8	22	1	5	0,75	3	2	0,197	2,48	3,03	13,8
9	30	0,6	3	0,25	7	2			2,4	9,89
10	15	1	3	0,25	7	4	0,237	1,89	2,49	10,52
11	18	0,6	5	0,25	7	4	0,212	1,75	3,26	14,27
12	29	1	5	0,25	7	2	0,211	1,34	3,49	16,07
13	14	0,6	3	0,75	7	4			2,08	9,08
14	13	1	3	0,75	7	2	0,231	1,92	2,2	9,78
15	24	0,6	5	0,75	7	2	0,216	1,89	2,76	12,92
16	16	1	5	0,75	7	4	0,211	1,43	2,84	14,1
17	27	0,4	4	0,5	5	3			2,51	
18	5	1,2	4	0,5	5	3	0,199	1,90	2,98	13
19	20	0,8	2	0,5	5	3			1,82	7,36
20	17	0,8	6	0,5	5	3	0,200	1,73	3,5	16,04
21	7	0,8	4	0	5	3	0,214	2,13	3,27	13,25
22	19	0,8	4	1	5	3	0,230	2,21	2,36	10,9
23	23	0,8	4	0,5	1	3	0,199	3,63	2,98	11,62
24	9	0,8	4	0,5	9	3	0,220	1,60	2,73	12,35
25	4	0,8	4	0,5	5	1	0,210	2,26	2,81	11,95
26	31	0,8	4	0,5	5	5	0,240	2,12	2,64	11,76
27	11	0,8	4	0,5	5	3	0,215	2,16	2,72	11,88
28	10	0,8	4	0,5	5	3	0,222	2,22	2,82	12,06
29	6	0,8	4	0,5	5	3	0,214	2,17	2,71	11,95
30	1	0,8	4	0,5	5	3	0,210	2,17	2,72	11,83
31	21	0,8	4	0,5	5	3	0,230	2,23	2,79	12,02
32	32	0,8	4	0,5	5	3	0,235	2,21	2,76	11,89

The experiments could be run in sequence since no change of membrane or spacer was needed. To monitor that no drift or carry-over occurred in the system the center points were used as system suitability tests (SSTs) and runs with only buffer injected were used as blanks. As can be seen from Figure 9, 10 and 11, no significant drift or carry-over occurred.

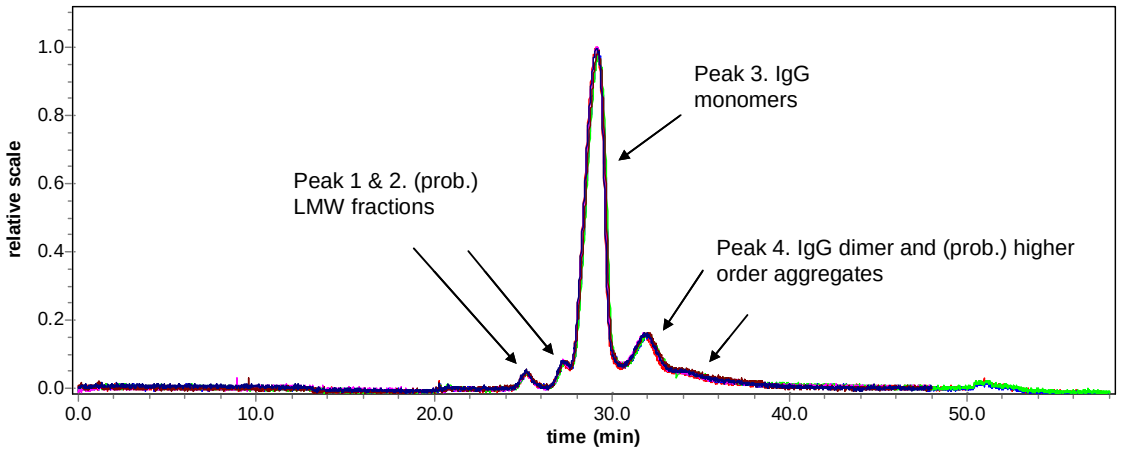

Figure 9. *Comparison between 6 identical SST-runs done within 38 experiments show that there is no significant drift/reproducibility problem in the system. Peak 1 and 2 are thought to be fractionated antibodies, but because of their low abundance it has not been possible to determine their mass. Peak 3, the main peak, are IgG monomers with an estimated molar mass of 156 kDa. Peak 4 consist of IgG dimers, 310 kDa, and probably larger higher order aggregates. The molar masses were estimated for Exp No 24 in the optimization experimental set using data from the RI and MALS detectors.*

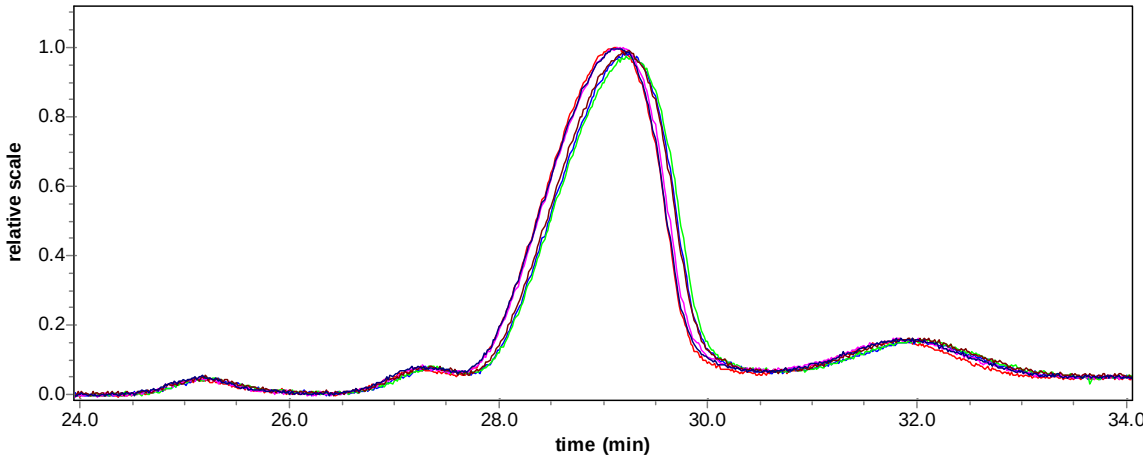

Figure 10. *When zooming in the main peak of Figure 9, the impression is first of two series with a small difference between them. However, closer inspection shows no systematic variance. The difference between the foremost and the latest peak is about 8 seconds.*

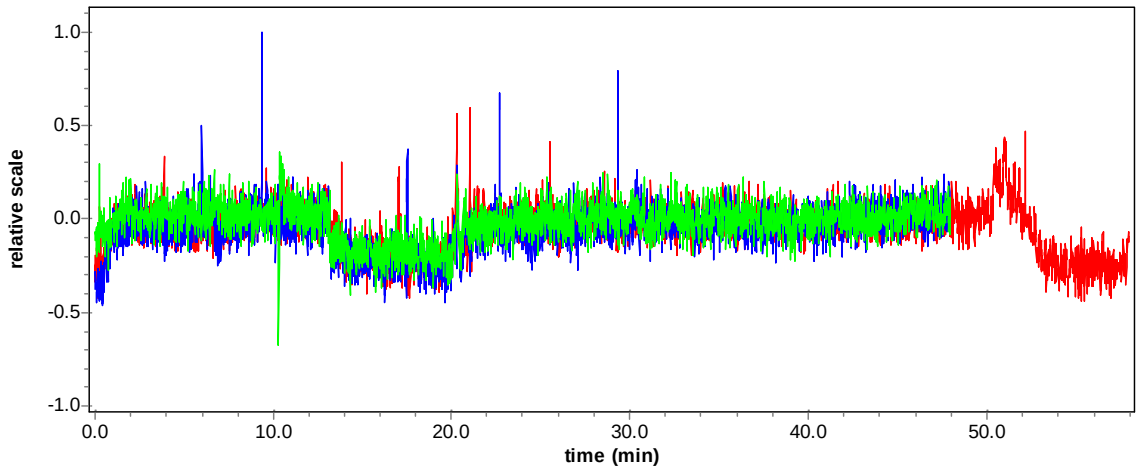

Figure 11. *Comparison of 3 blank samples with 38 samples in-between them show that there is no carry-over between runs. However, the signal is weakly flow dependent, while a different flow during t=13-20 shows a small change in baseline. For a reference to the scale used please compare with the baseline in Figure 9.*

3.1.2.1 Percentage of Aggregation Response

The Percentage of Aggregation response reports the amount of the sample found in peak 4, the dimer peak. In the replicate plot for the response, Figure 12, the range is from 19 % to 24 % with a statistically normal distribution between high and low values. The replicated center points are generally situated above average, indicating some curvature.

The spread of the replicates are quite large, between 21-23.5%. This is intriguing since the SSTs showed so high correlation. It is possible that part of the variation can be explained by difficulty in measuring the responses rather than actual difference. The dimer peak trails markedly and how much of this trail is regarded as part of the peak as well as variations in setting the baseline could affect the measurement. In Figure 12 b) the replicates are numbered in the order they were measured. This show a trend towards higher responses, possibly reflecting evolving practice when, manually, determining the response.

A model was fitted with MLR using 26 experiments. Figure 13 show the actual measured values plotted against the values predicted by the model. The spread of the replicates is fairly big, but still a clear trend can be seen. The R2 is 0.828 and Q2 is 0.681. This means that the model is **valid**.

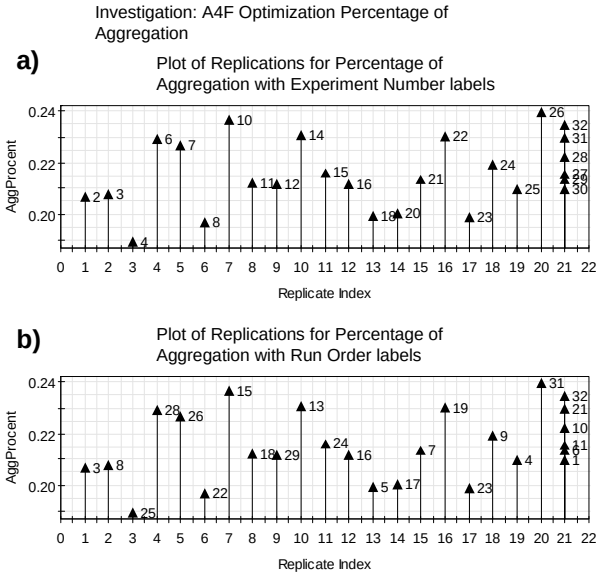

Figure 12. *Replicate plot for Percentage of Aggregation response.* ***a)*** *Experiment number labels.* ***b)*** *Run order labels.*

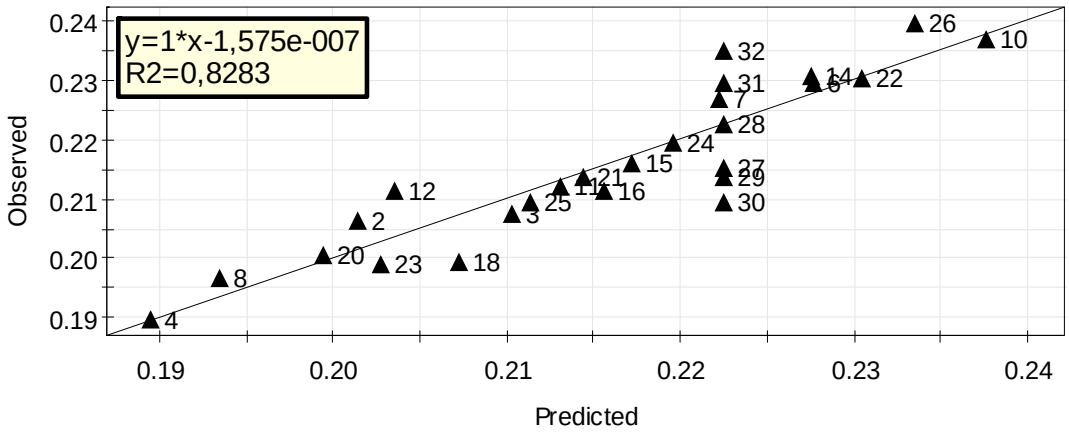

Figure 13. *Observed versus Predicted plot for the Percentage of aggregation response. Dots are labelled with experiment numbers. N=26, DF=17, R2=0.828 and Q2=0.681.*

It is possible that the model only illustrates the difficulty in measuring the aggregate levels even though the model is deemed to be valid. The coefficient plot seen in Figure 14 indicates that increasing channel flow (Vc) and crossflow to channel flow ratio (Vx/Vc) should give less aggregates. This is contrary to expectations. Increasing Vc and Vx/Vc give a higher concentration of the sample close to the ultra-filtration membrane. A higher local concentration of the sample should reasonably rather induce more aggregates. However, a decrease in Vc and Vx/Vc generally give broader peaks. Possibly this could influence the carry-over of the main peak into the dimer peak, resulting in a seemingly higher dimer distribution.

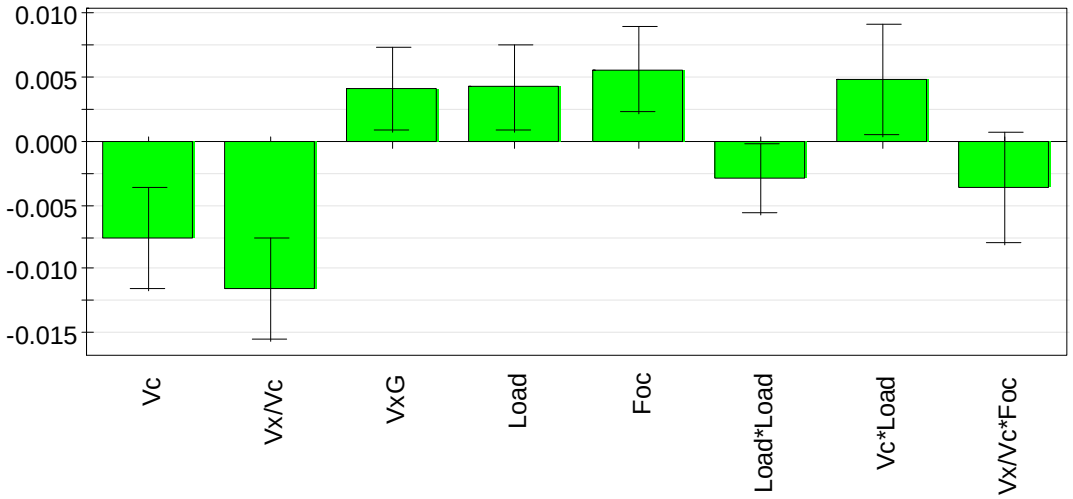

Figure 14. *Coefficient plot for the Percent of aggregation model. Vc – Channel flow, Vx/Vc – Crossflow to channel flow ratio, VxG – Crossflow gradient, Load – Sample load, Foc – Focus time. The error bars indicate a confidence level of 95 %. N=26, DF=17, R2=0.828 and Q2=0.681.*

3.1.2.2. Resolution Between Peaks 4 and 3 Response

The replicate plot for the resolution response shows a normal distribution between the samples, see Figure 15. The replicated center points are situated a little bit above the average response, indicating weak curvature. They are also well gathered, indicating a low error in the measurements.

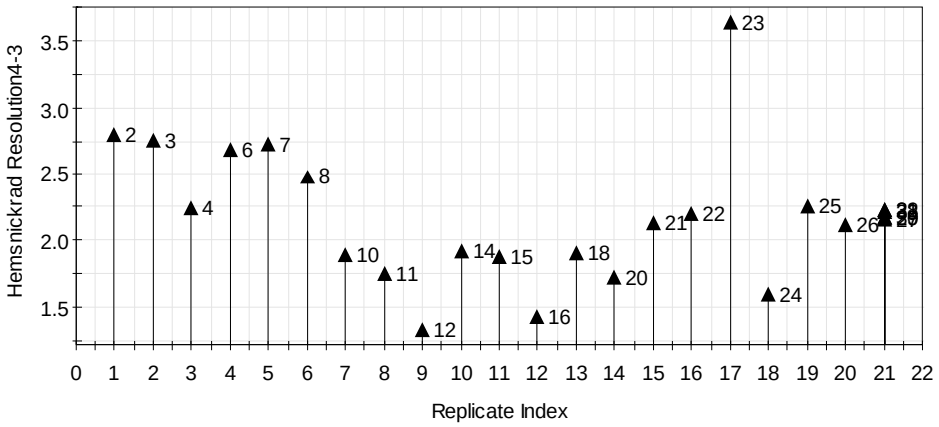

Figure 15. *Replicate plot for the resolution response. Bars are labelled with experiment numbers, replicates are overlaid in the same bar.*

The model was fitted with MLR using 26 experiments. The observed versus predicted responses show a high grade of correlation as is shown in Figure 16. The R2 and Q2 values are excellent, 0.983 and 0.967 respectively, indicating that the model is **valid**.

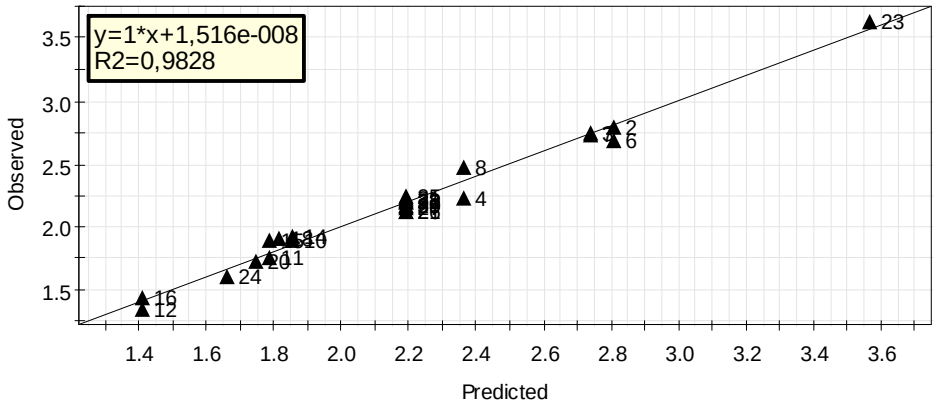

Figure 16. *Observed versus predicted plot for the resolution response. Dots are labelled with experiment numbers. N=26, DF=21, R2=0.983 and Q2=0.967.*

Even though the model is valid, the measure is not necessarily ideal for this optimization. The coefficient plot in Figure 17 indicates that low channel flow and crossflow to channel flow ratio values would give a better resolution response. This is contrary to expectations, usually the opposite is true. The negative impact of sample load on resolution was as expected though.

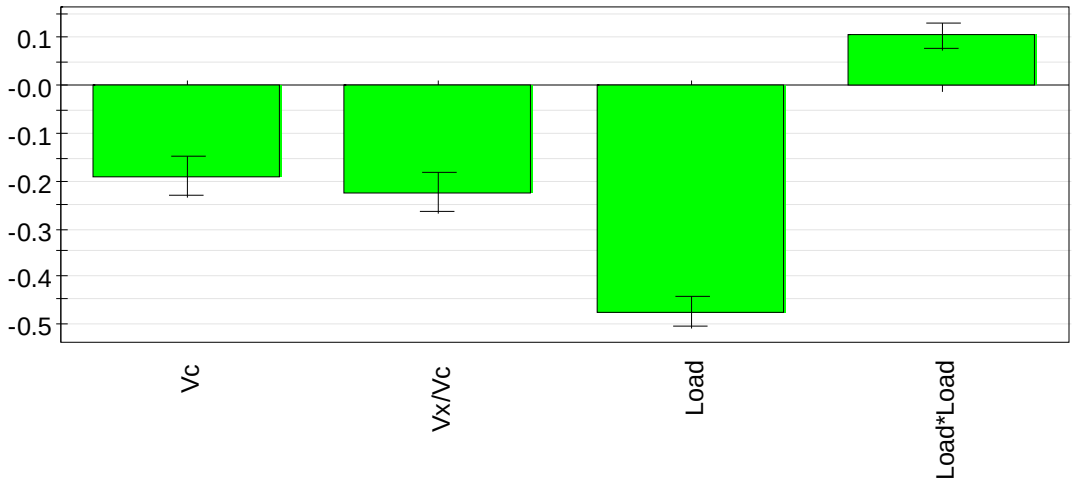

Figure 17. *Coefficient plot for the resolution between peaks 3 and 4 model. The negative impacts of Vc and Vx/Vc are contrary to expectations, while the negative impact of sample load was expected. The error bars represent a 95 % confidence level. N=26, DF=21, R2=0.983 and Q2=0.967.*

To investigate the influence of the channel flow (Vc) and the sample load (Load) an SST and the high axial points for these settings were compared in Figure MM. The run with the high Vc, Figure 18 b), should according to the model have a worse resolution between peaks 3 and 4. This is mainly because the main peak becomes broader with higher Vc, even though the separation between peaks is at least as good as with a lower Vc.

It is possible that the high Vc causes the different monomer species in the antibody mixture to start to separate, leading to a broader peak. If so, the same would be true for the Vx/Vc-effect; a higher separation pressure causes the monomer peak to broaden, resulting in a better resolution score. The comparison between Figure 18 a) and c) shows that increased sample load leads to broader peaks and no improved separation, and therefore a worse resolution score.

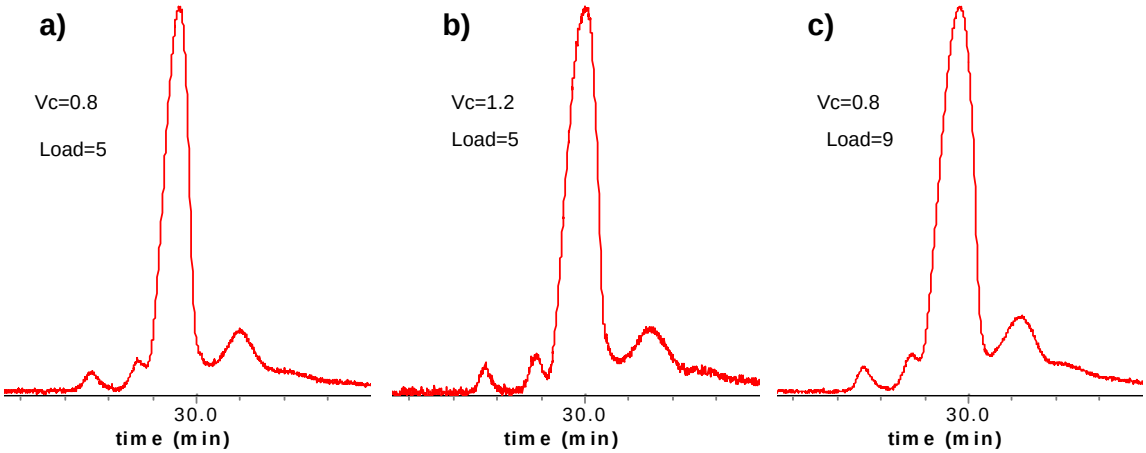

Figure 18. *Separation comparison between an SST and high axial point settings for two of the coefficients in the resolution model.* ***a)*** *SST run.* ***b)*** *High setting for Vc.* ***c)*** *High setting for Load.*

3.1.2.3. Difference in Retention Time Between Peaks 3 and 4 Response

The resolution model was not able to satisfactorily describe a good separation. The problems were found to be mainly related to the peak broadness. A broad peak led to a bad response even though the separation was not necessarily bad. The Difference in retention times of peak 3 and 4 response, ΔRt43, was achieved by simply removing the peak width influences from the resolution measure.

The replicate plot for ΔRt43, Figure 19, shows a normal distribution of the responses over a range of 1.8 to 3.5 minutes. The center point replicates are tightly distributed in the middle of the range, pointing to low measurement errors and low influence of curvature.

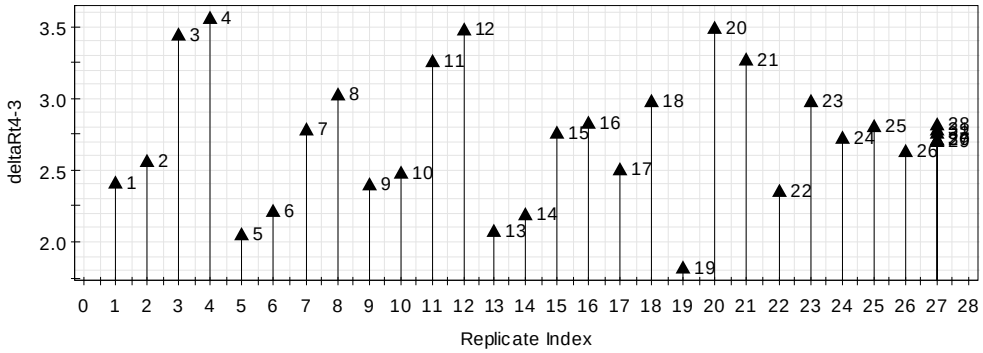

Figure 19. *Replicate plot for ΔRt43. Bars are labelled with experiment numbers, replicates are overlaid.*

The model was fitted with multiple linear regression, MLR, using all 32 experiment points. The responses predicted by the model closely followed the values actually measured, see Figure 20. Because of the high R2, 0.991, and Q2, 0.981, the model is deemed **valid**.

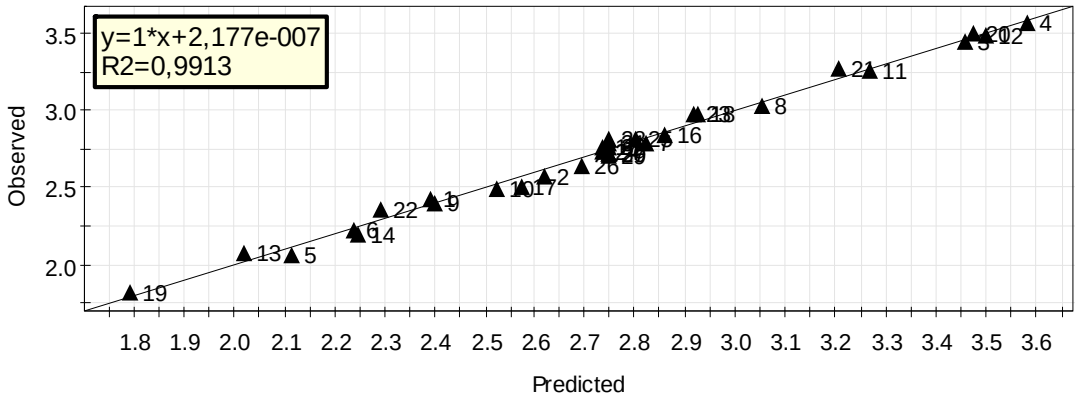

Figure 20. *Observed versus predicted plot for ΔRt43. Both the R2 and the Q2 are very high, indicating an accurate model. Dots are labelled with experiment numbers. N=32, DF=22, R2=0.991 and Q2=0.981.*

The model coefficients, shown in Figure 21, clearly indicate that the crossflow to channel flow ratio (Vx/Vc) and the crossflow gradient (VxG) are the most important variables for ΔRt43. This is also in line with literature. Wahlund and Giddings (1987) show that, given our variables, the retention time is theoretically almost exclusively dependent on Vx/Vc. VxG is a moderator of how Vx/Vc changes over time in the separation.

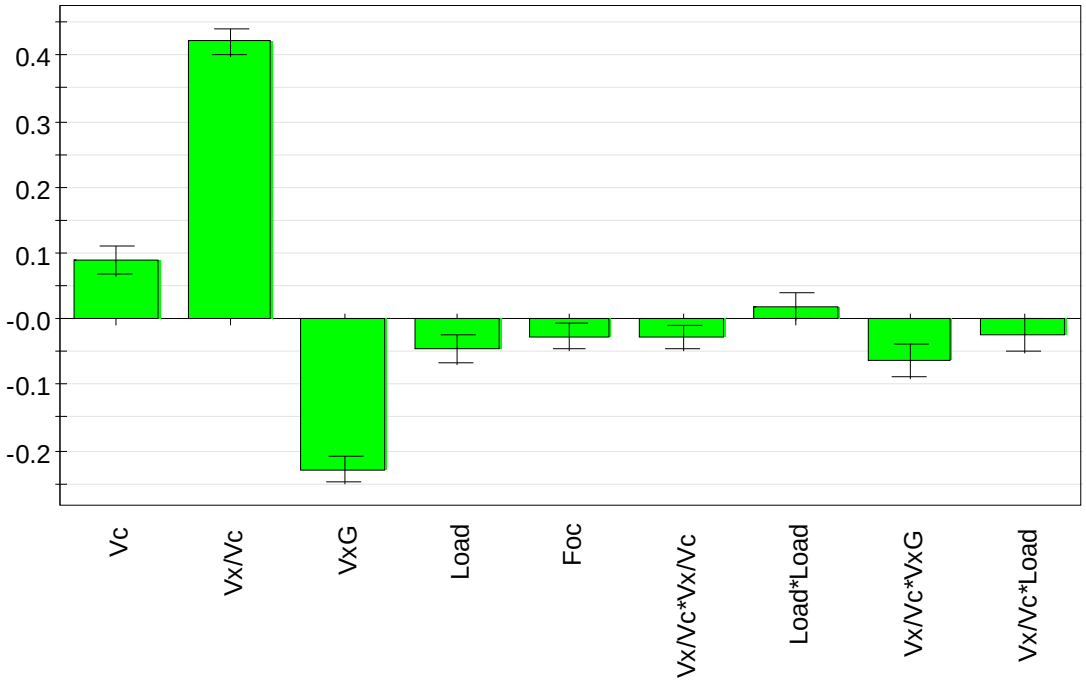

Figure 21. *Model coefficients for the ΔRt43 response. Error bars represent a 95 % confidence level. N=32, DF=22, R2=0.991 and Q2=0.981.*

3.1.2.4. Retention Time for Peak 4 Response

It is desirable both that analysis runs deliver good results and that they are quick. To predict the analysis time for this sample a response, Rt4, was introduced that simply measured the retention time for the last peak, peak 4. This response could be used as a border condition in an optimization.

The replicate plot, Figure 22, shows a range from 7 up to 16 minutes. The distribution seems fairly normal with replicated center points tightly grouped in the middle of the range. A pairwise distribution pattern reveals already that the second variable in the experiment design matrix, Vx/Vc, heavily influences the response.

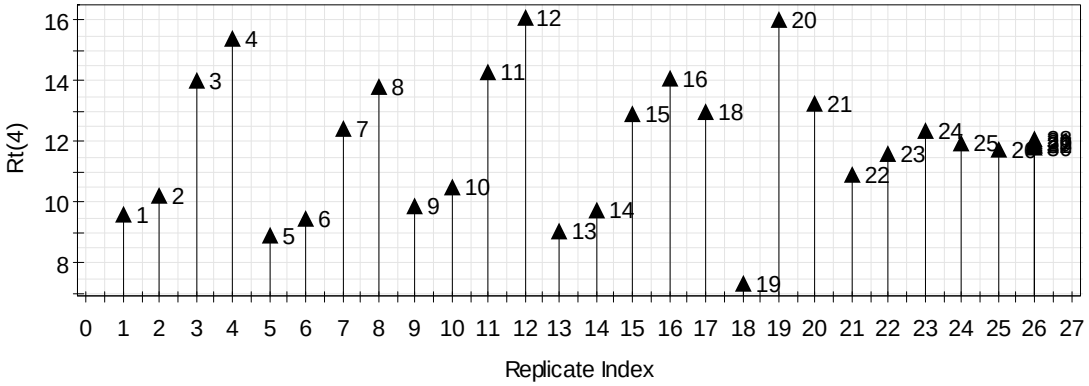

Figure 22. *Replicate plot for peak 4 retention time. Bars are labelled with experiment numbers and replicates are overlaid.*

The model was fitted with MLR using 31 experiment points. The responses predicted by the model show a very high accordance with the observed responses, see Figure 23. The R2/Q2 of 0.997/0.995 is extremely high, again indicating a very good fit and that the model is **valid**.

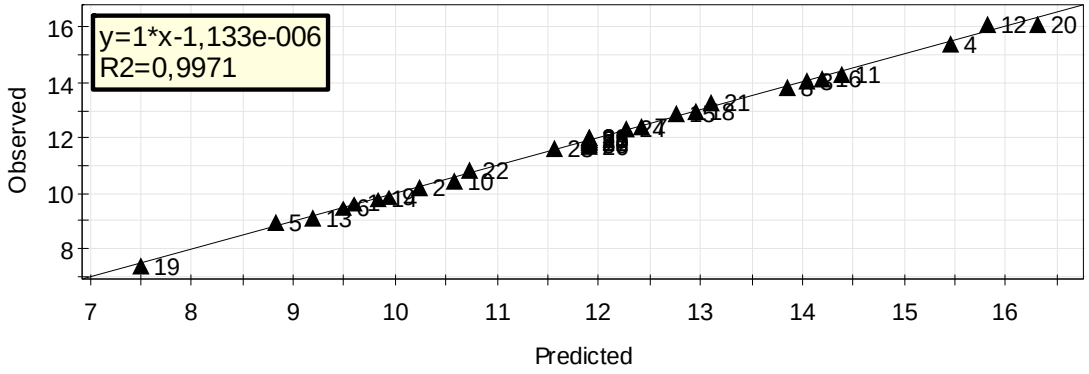

Figure 23. *Observed versus predicted responses for peak 4 retention time. Dots are labelled with experiment numbers. N=31, DF=24, R2=0.997 and Q2=0.995.*

When constructing the model a weak outlier was identified using a normal probability plot of residuals, see Figure 24. This outlier was deleted and was not incorporated in neither the

model nor the replicate plot above. The experiment deleted was an axial point with a very low channel flow. It is possible that the low channel flow somehow affected other parameters such as the crossflow, resulting in a slightly disturbed response.

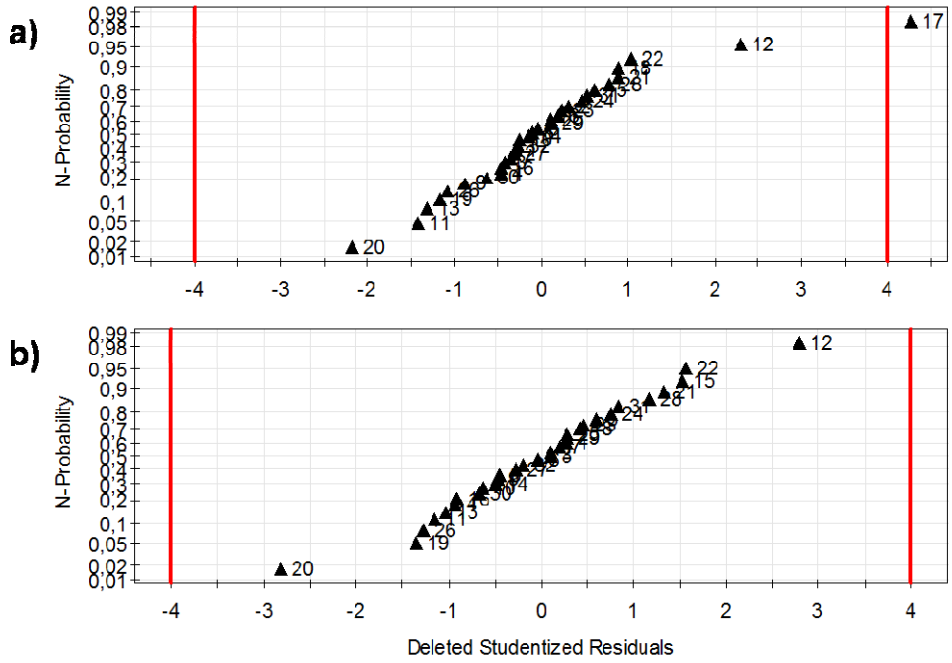

Figure 24. *Experiment 6 was detected as an outlier with this normal probability plot of the residuals. The deletion of the outlier had a marginal impact on the model, R2/Q2 raised from 0.995/0.991 in a) to 0.997/0.995 in b).*

The model coefficients confirm, as in the ΔRt43 response, a strong dependence of Vx/Vc and VxG, see Figure 25. The third most important factor is Vc, which also corresponds well with personal experience.

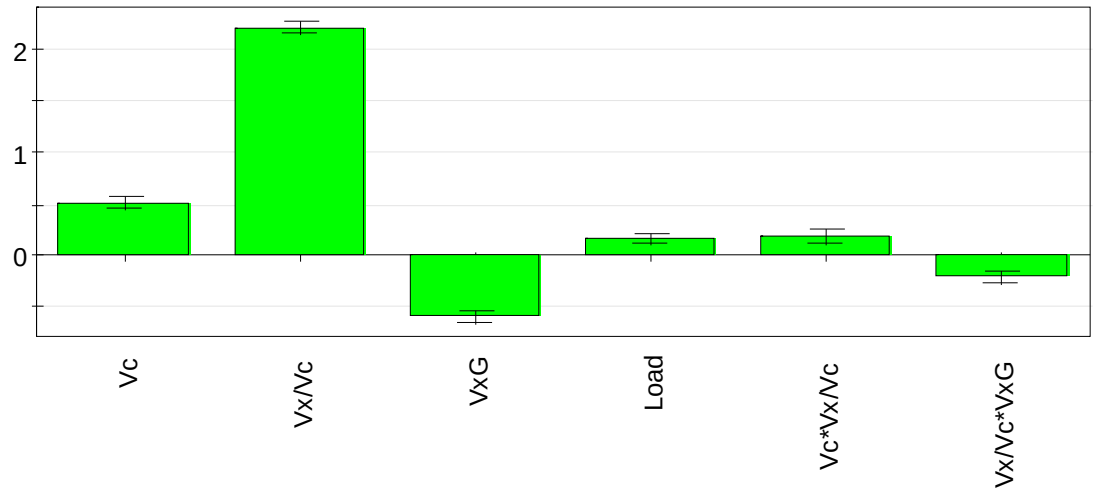

Figure 25. *Coefficient plot for the Rt4 model. Error bars indicate a 95 % confidence level. N=31, DF=24, R2=0.997 and Q2=0.995.*

It can be noted that even though very small sample amounts were used, 1-9 µl corresponding to 0.73-6.57 µg, the sample load still slightly affects the retention time. This seems to be because the channel very easily becomes slightly overloaded. Too much sample results in clearly fronting peaks that have their peak maximum slightly delayed, see Figure 26.

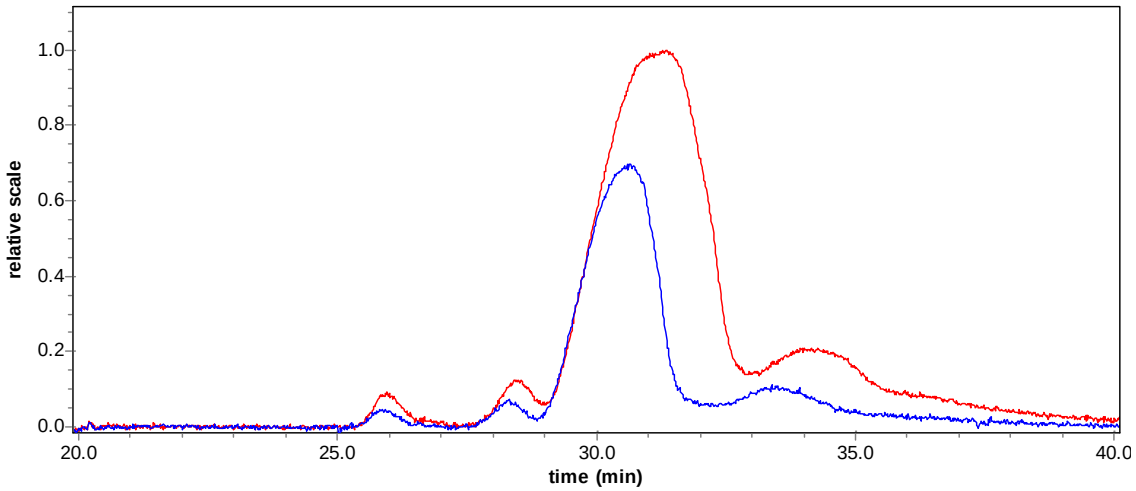

Figure 26. *The effect of sample load on retention time. A higher sample load delays the peak maximum. Overlay of two runs with identical settings except that the larger peak, 10 µl, has twice the sample load of the smaller peak, 5 µl.*

3.2. New Method Development

As part of the study a new and optimized method for separating the antibody mixture was developed. A criterion for the optimized method was that it should be capable of separating LMW impurities, though focus was on the separation of the monomer and the aggregate peaks. The new method is based on data taken from the DoE optimization experiments.

In the DoE trial no definite response could be determined that would yield the optimal separation though. To develop the new method a starting point was taken in the response that modelled the difference in retention time between the monomer and the aggregate peaks (ΔRt43). This was complemented with an effort to sharpen the peaks and to keep the total retention time acceptably low.

The coefficients for the ΔRt43 model were previously shown in Figure 21. Below chromatograms for the axial point experiments are presented and discussed in order to get a visual appreciation of the effects of the different parameters.

The ΔRt43 model suggests that a low crossflow gradient (VxG) would yield a higher ΔRt. This is fairly intuitive, a lower VxG means a higher average crossflow rate and also a relatively higher average crossflow for the later peak, resulting in both a prolonged separation and an increase in ΔRt. However, as can be seen in Figure 27 it doesn't necessarily result in a better separation. Although the separation between peak 2 and the main peak might be slightly poorer, the overall separation is generally better for a high VxG with sharper and more distinct peaks. The total separation time is also faster.

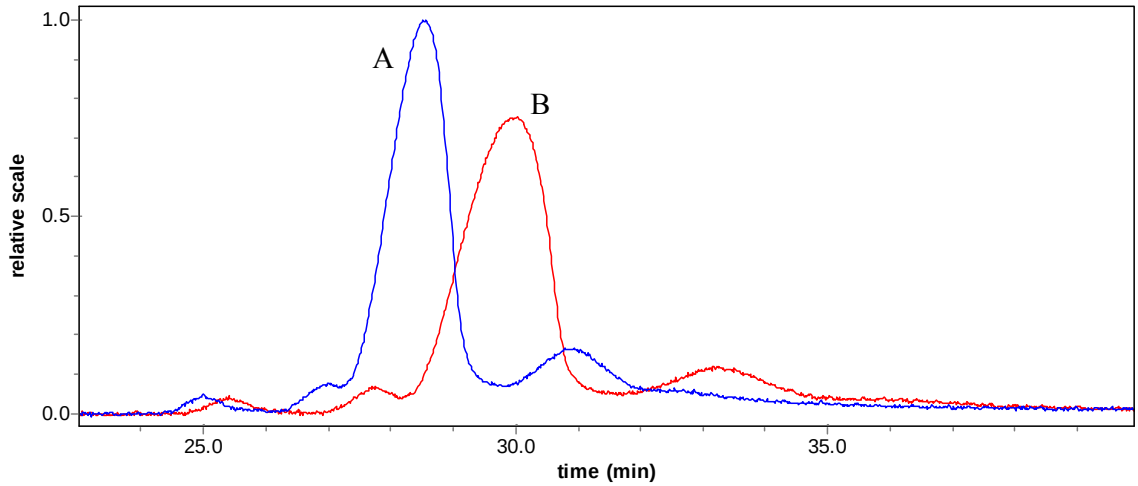

Figure 27. *Crossflow gradient comparison. Run A has a high crossflow gradient (VxG=1) – the crossflow is reduced to zero at the end of the run, run B has no gradient – the crossflow is constant over the entire run.*

The most important coefficient in the ΔRt43 model is the crossflow to channel flow ratio (Vx/Vc). In Figure 28 a run with Vx/Vc=2 is compared to a run with Vx/Vc=6. The high Vx/Vc run show a higher separating power, distinctly separating the LMW peaks. However, it also causes the main peak to broaden and a longer total retention time.

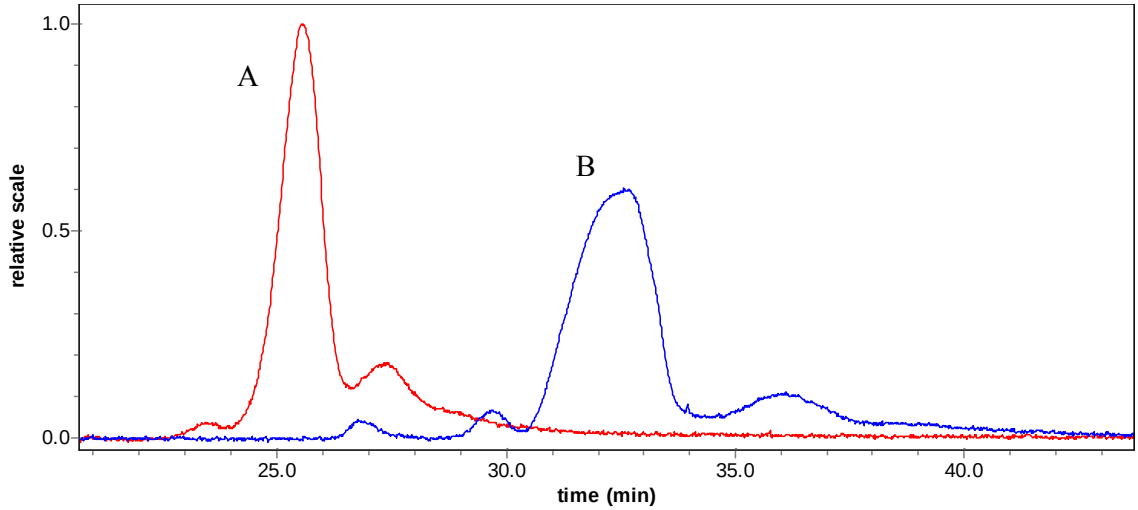

Figure 28. *Vx/Vc comparison. A low Vx/Vc ratio, for run A Vx/Vc=2, gives an earlier elution time but worse a separation than a high ratio (B, Vx/Vc=6).*

An increased channel flow (Vc) give a better separation but a higher noise level because the sample passes the detector faster, see Figure 29. Given a constant Vx/Vc ratio a higher Vc only slightly affects retention times.

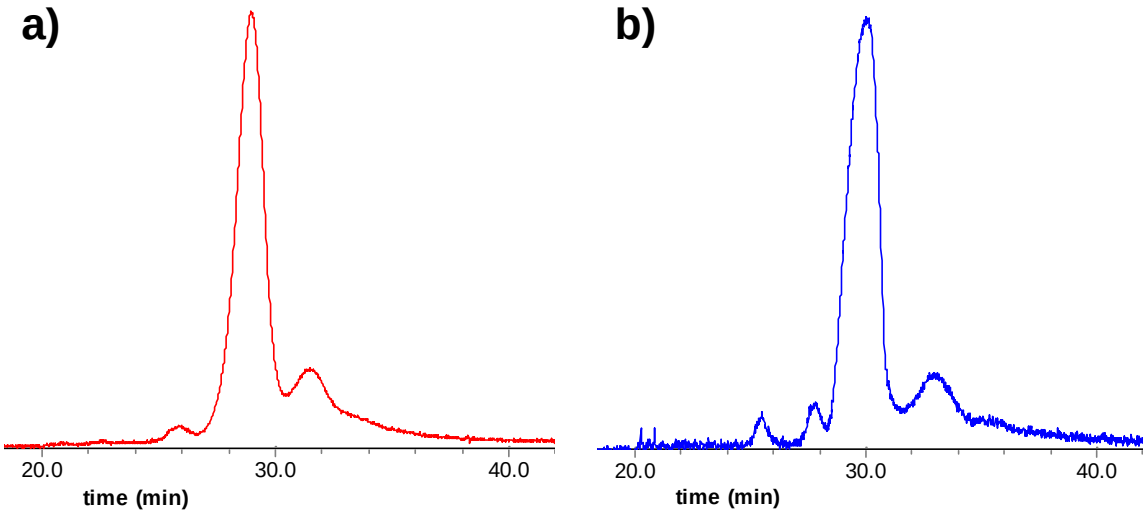

Figure 29. a) *Channel flow Vc=0.4 ml/min.* ***b)*** *Vc=1.2 ml/min. An increased channel flow gives a better separation but a higher noise level.*

An increased focus time gives a marginally better separation, see Figure 30.

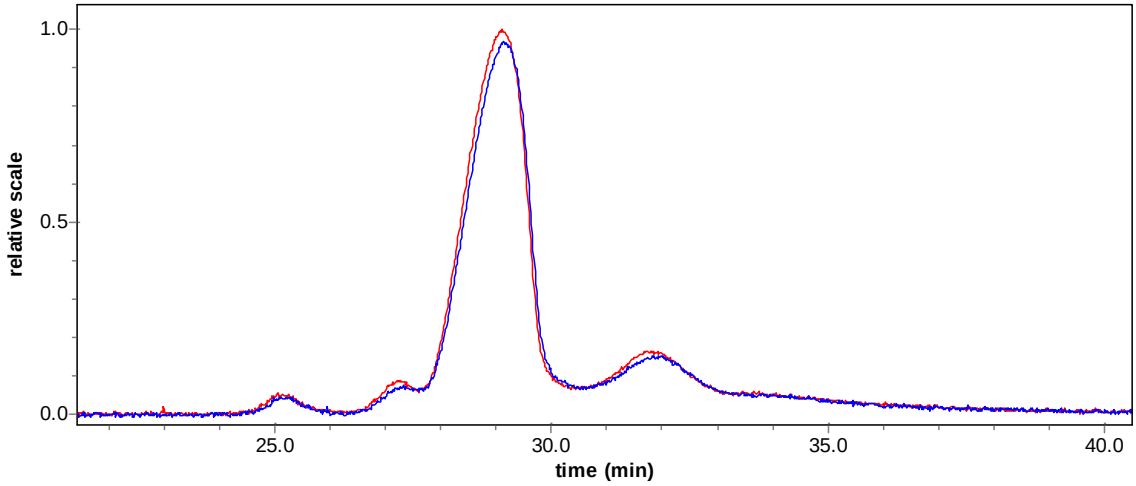

Figure 30. *Blue chromatogram has a focus time of one minute; red chromatogram has a focus time of five minutes. Red has marginally more distinct peaks.*

A low sample load gives narrower peaks but a higher signal to noise ratio, see Figure 31.

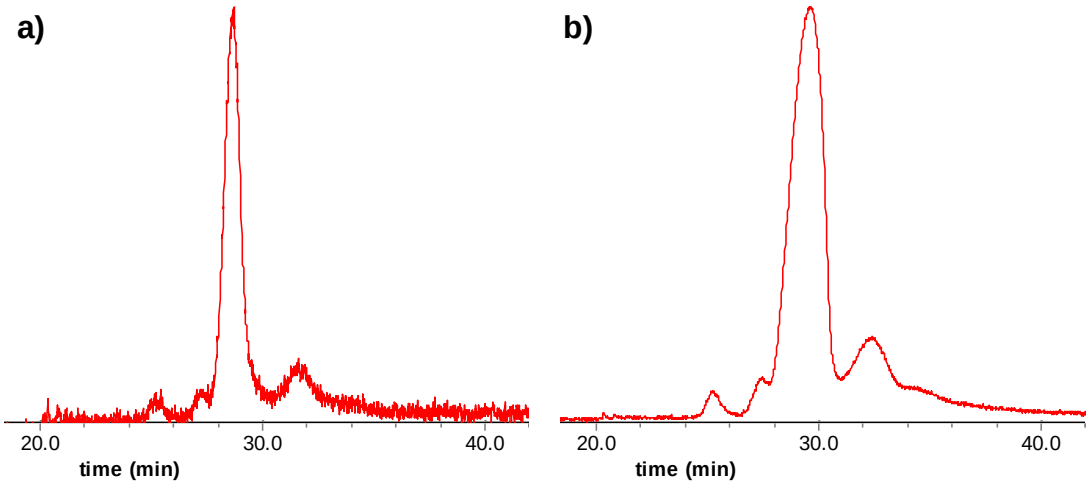

Figure 31. a) *Sample load is 1 µl.* ***b)*** *Sample load is 9 µl. A low sample load gives narrower peaks but a higher signal to noise ratio.*

Considering the data presented above an optimized elution scheme was developed, as shown in Table 11. A variant scheme for sequential mode use is also shown in Table 12, here the equilibration step is prolonged. Step one is an equilibration step to help to obtain a baseline. In step 2-4 the channel is run in focus flow mode. Step 2 is only there to obtain a stable focus flow before step 3 when the sample is injected. Here a focus time of three minutes was chosen. Step 4 is only an additional focus step, this time without any potentially disturbing injection flow. Step 5 is the actual elution step. A channel flow of 1 ml/min was chosen with a Vx/Vc ratio of 5 and with a 0.75 gradient down to 1.30 ml/min (should technically be 1.25 but the program rounds this to 1.30). Finally, step 6 is a rinsing step that purges the channel and membrane, 10 minutes was found to be appropriate for this.

Table 11. *Optimized antibody mixture separation scheme.*

Flowrate:	1 ml/min	**Channel:** Long		**Spacer:** 350M	
Step	**delta t**	**Time**	**Mode**	**X start**	**X end**	**Focus Flow**
1	3.00	3.00	Elu	5.00	5.00	-
2	2.00	5.00	Focus	-	-	2.00
3	3.00	8.00	Foc+Inj	-	-	2.00
4	2.00	10.00	Focus	-	-	2.00
5	30.00	40.00	Elu	5.00	1.30	-
6	10.00	50.00	Elu+Inj	0.00	0.00	-

Table 12. *Optimized antibody mixture separation scheme for* sequential *runs.*

Flowrate:	1 ml/min	**Channel:** Long		**Spacer:** 350M	
Step	**delta t**	**Time**	**Mode**	**X start**	**X end**	**Focus Flow**
1	*8.00*	8.00	Elu	5.00	5.00	-
2	2.00	10.00	Focus	-	-	2.00
3	3.00	13.00	Foc+Inj	-	-	2.00
4	2.00	15.00	Focus	-	-	2.00
5	30.00	45.00	Elu	5.00	1.30	-
6	10.00	55.00	Elu+Inj	0.00	0.00	-

3.3. Correlation Studies

The purpose of these studies is both to compare actual results obtained by different techniques and to describe various merits and drawbacks of them. The SE-HPLC method is not able to separate low molecular weight fractions from the monomer peak. Therefore, to get an accurate comparison when correlating the results of the SE-HPLC, A4F and AUC runs, LMW fractions will be included in the monomer/main peak.

3.3.1 Asymmetrical Flow Field-Flow Fractionation

The aggregated AbM sample was run with the optimized method. An example chromatogram can be seen in Figure 32 and the result based on two runs in Table 13.

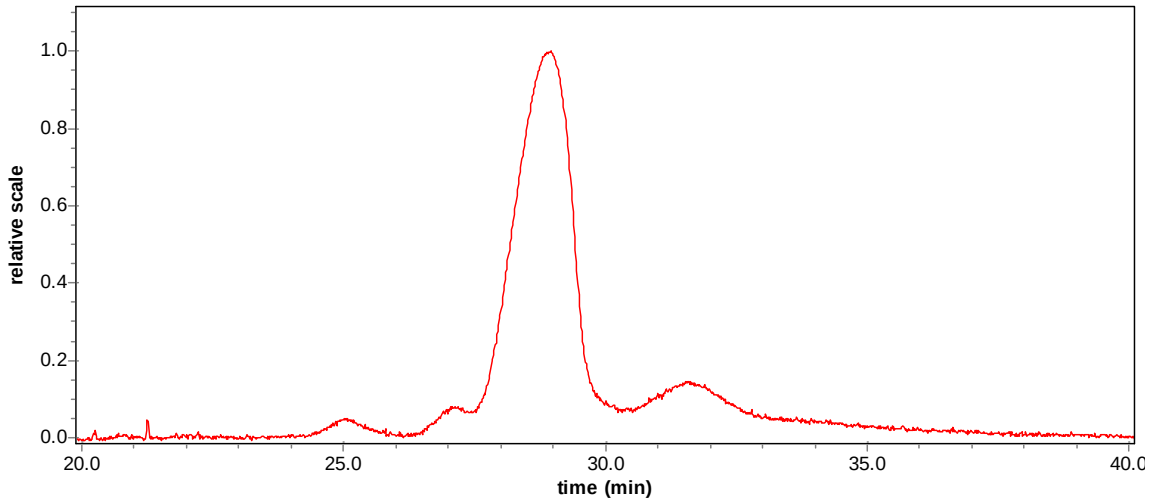

Figure 32. *Aggregated antibody mixture sample run with A4F optimized method.*

	Monomer	Aggregate
Run14	78,5%	21,5%
Run8	78,4%	21,6%
Mean	78,4%	21,6%

3.3.2. Dynamic Light Scattering

In the DLS measurements a slightly different sample was used. However, the only thing that differed was a 3h UV-irradiation time, compared to 4h for the other samples. The aggregate content is also around 75% of the 4h sample. Figure 33 show the light scattering intensity (measured at 90°) during 10 second long acquisition intervals. All shown data points were used in the calculation of the Correlation function presented in Figure 34.

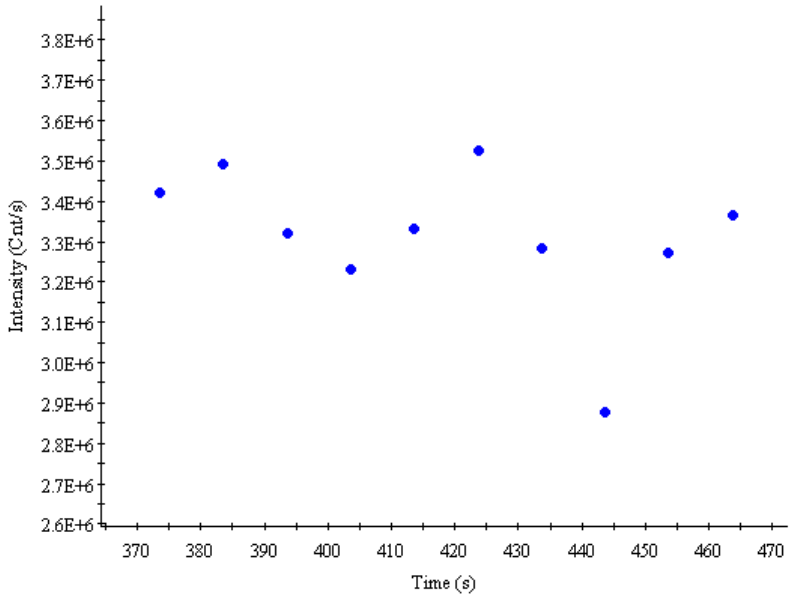

Figure 33. *Total intensity in 10, 10 second long acquisitions. The sample is considered to be in PBS.*

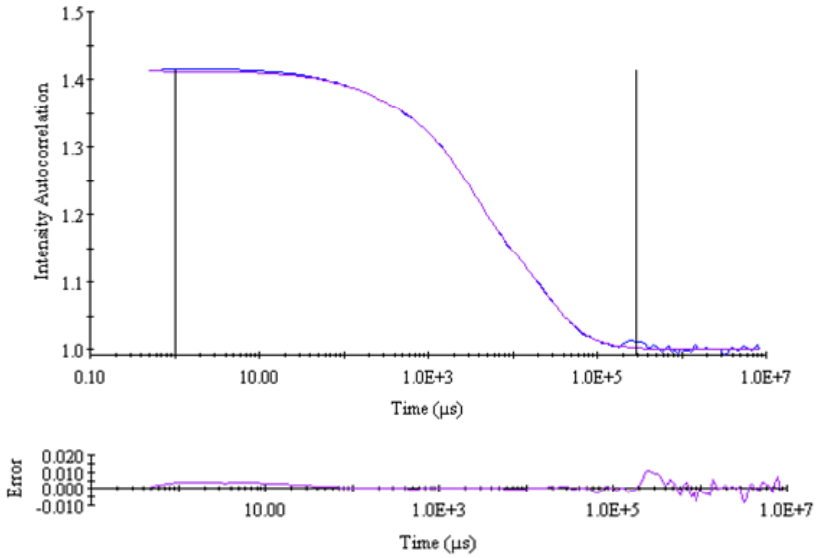

Figure 34. *Correlation function of sample.*
Blue trace – experimental autocorrelation light scattering intensity fluctuation function (correlation function). Magenta trace – approximation with a sum of exponential functions. Lower panel – residuals. Note logarithmic time scale.

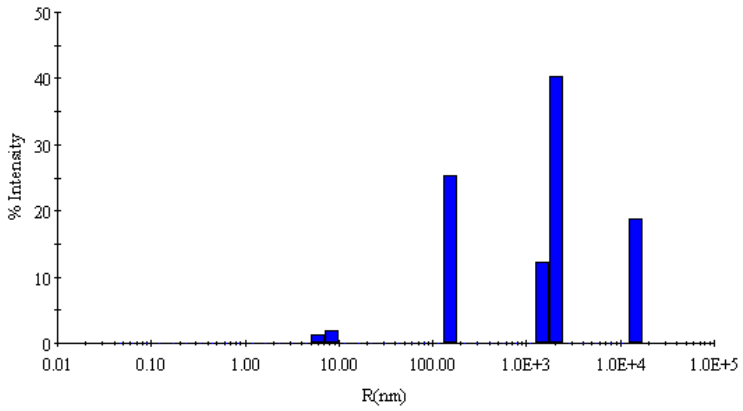

Item	R (nm)	%Pd	MW-R (kDa)	%Int	%Mass
Peak 1	7.4	15.3	369	3.4	75.7
Peak 2	155.7	0.0	453408	25.4	0.2
Peak 3	1953.5	12.5	168656000	52.5	6.8
Peak 4	14632.2	0.0	18757400000	18.8	17.3

Figure 35. *Light scattering particle size distribution diagram for the UV treated AbM sample obtained from the correlation function in Figure VV.*
Note: Calculations of R were made assuming a spherical form of the light scattering particles that were considered to be in PBS buffer. Viscosity = 1.019 cp at 20 °C was automatically corrected for the temperature of the measurements 25 °C.

The calculated results of the DLS measurement is presented in Figure 35. The data is presented in a different way than for A4F since the sample is analyzed in a batch. Peak 1 corresponds to the monomer/dimer species, peak 2 could be high molecular weight aggregates, peak 3 and 4 are probably dust particles.

As can be seen in the corresponding table an estimated 75.7 % of the mass in the sample are from the dimer/monomer species. The other peaks can not be compared to results from other techniques, since they don't have the same range as DLS. This range comes at a cost though, DLS cannot separate the monomer and the dimer species which renders it useless for this application. It is possible to increase the resolution of DLS by carefully filtering the sample through an ultrafiltration membrane with a, for example, 0.2µm pore size. Even after careful filtration it is still only possible to distinguish large trends in the monomer/dimer distribution, an example can be seen in Figure 36.

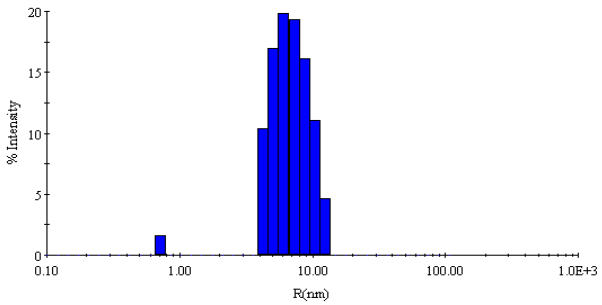

Figure 36. *Size distribution diagram for a filtered UV treated AbM sample.*

3.3.3. Native Polyacrylamide Gel Electrophoresis

Three samples were run with native PAGE, each sample with two different concentrations. The gel from the experiment is shown in Figure 37 along with the indicated lane areas. The results are calculated from the amount of staining in the lane areas. Below the results from lanes 1 and 2 are discussed. The first contains the aggregated antibody mixture and the second contains an un-aggregated sample.

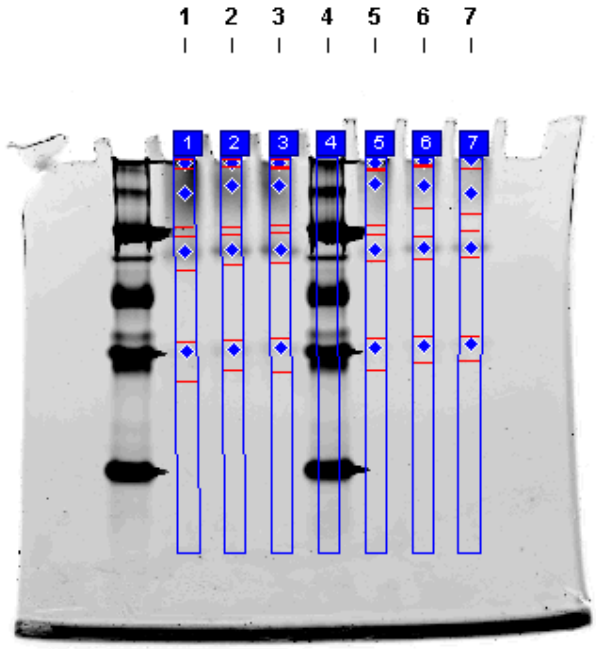

Lane	Bands	Band Volume	Lane Volume
1	4	153,735,905.96	163,751,239.18
2	4	97,497,462.20	102,003,766.60
3	4	92,867,074.90	99,648,482.85
4	0	0.00	446,854,656.60
5	4	59,091,360.08	67,353,809.32
6	4	38,005,577.47	42,352,686.56
7	4	35,389,508.48	38,038,710.02

Figure 37. *Native PAGE gel with indicated lane areas. Lane 1 is an aggregated antibody mixture and lane 2 is an un-aggregated sample. In each lane four identified bands are indicated with red borders. The corresponding table show the calculated total intensity, the volume, of the lanes and their bands.*

The method run was not optimized for this sample, and it shows. Although four bands were marked the results are not very clear, see Figure 38. Bands 3 and 4 have fairly distinct peaks but band 2 is more of a smear than an sharp line, and band 1 describes the gel well wall and the species that has not even really entered the gel.

Although the results are very inconclusive it is still possible to make a few educated guesses. In native PAGE samples separate both because of the sieving effects of the gel and because of different electric charges on the proteins. It is possible that band 4 contains low molecular weight impurities. If so, however, here the results indicate that the LMW content is higher in the non-aggregated sample which is contrary to experience from runs with other techniques. It can also be that band 4 corresponds to an antibody species with a variable chain that makes the molecule more negatively charged than others. In this scenario it is natural that the peak diminishes when aggregated because of cross-linking with less mobile species. Band 3 could relate to one or more monomer species with a certain common charge. Band 2 seems to be a smear of many different species. Its high presence also in the un-aggregated sample indicates that it consist of monomer species with a relatively more positive charge than those in band 3. Band 2 and 1 are also the bands where nearly all aggregated species are likely to be found.

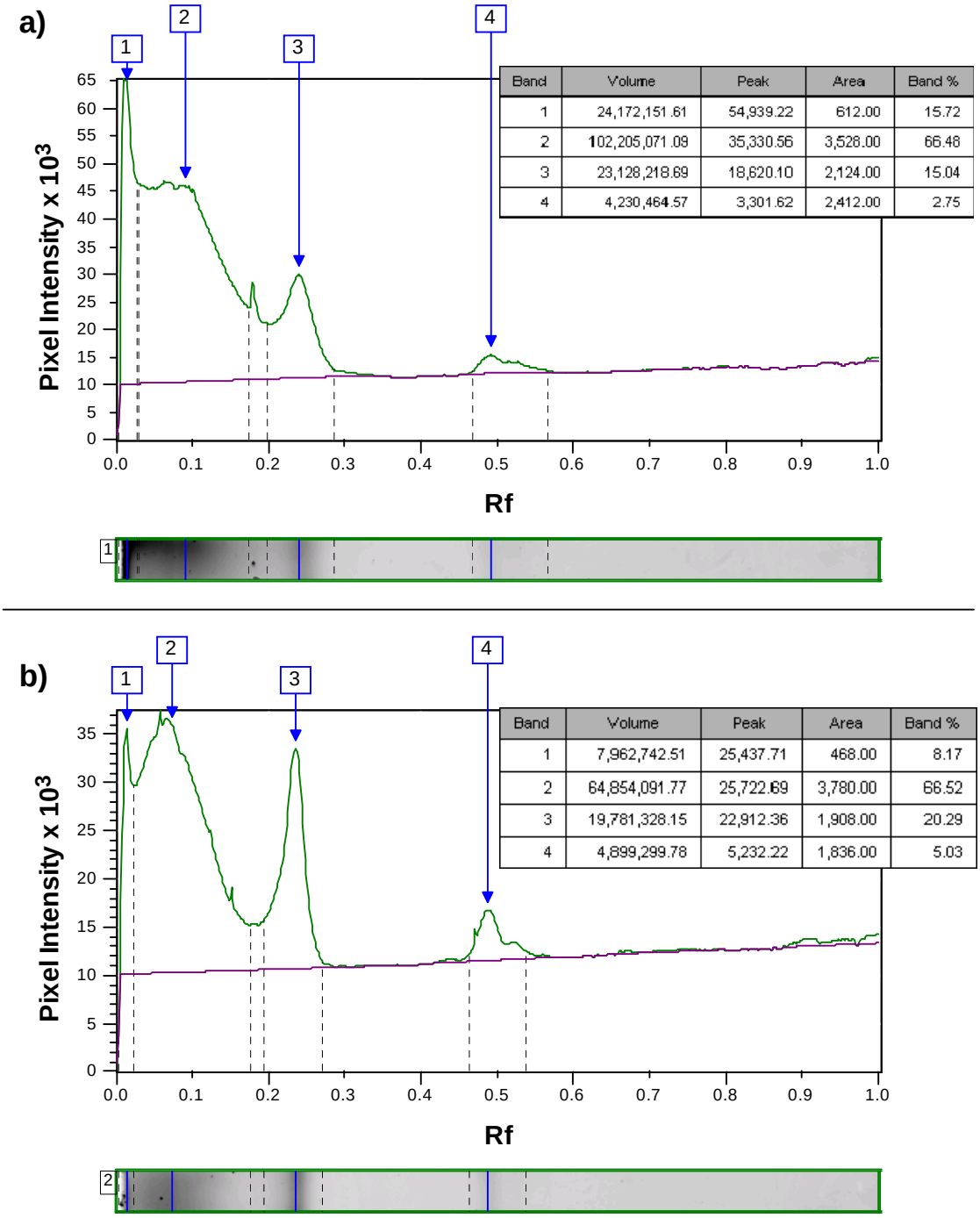

Figure 38. *Native PAGE gel lanes.* ***a)*** *Aggregated sample.* ***b)*** *Un-aggregated sample.*

It can be concluded that although Native PAGE has its uses for aggregate determination in homogenous protein samples, its use for this heterogeneous sample was of questionable value.

3.3.4. Sedimentation Velocity Analytical Ultracentrifugation

In this section historical data will be used since SV-AUC were not explicitly carried out as a part of this study. The data shown are based on a different preparation of the antibody mixture. Also here aggregates have been induced, though not covalently. From AUC data Figure 39 and Table 13 was constructed.

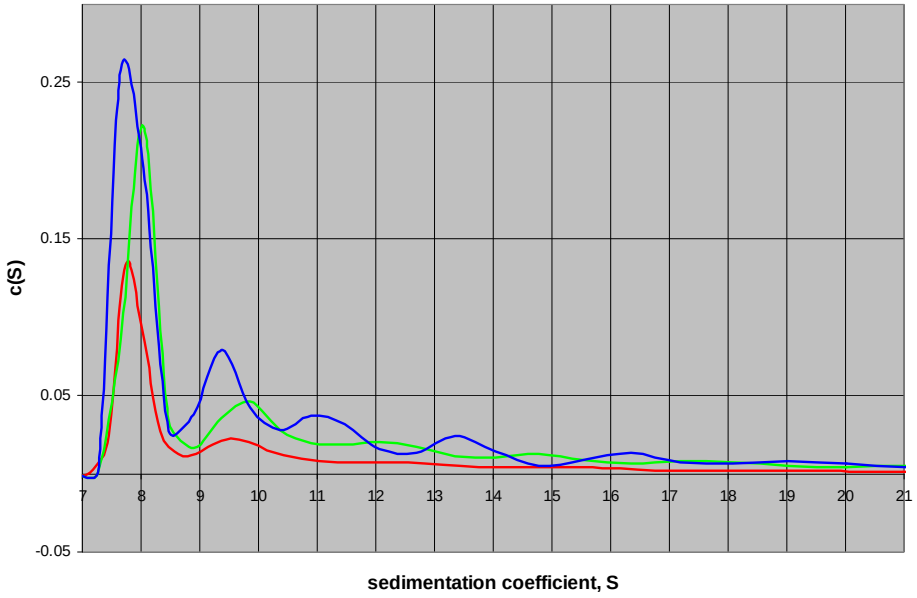

Figure 39. *Graph constructed from AUC data describing the monomer and aggregate species in a non-covalently aggregated sample. Table DD details the content of the blue sample which has the largest aggregate content.*

Table 13. *Table of the different species in a non-covalently aggregated antibody mixture sample. SV-AUC can quantify aggregate species down to tetramer level.*

Aggregated sample	S1	S2	S3	S4	S5	S6	S7	S8	S9	S10
Sedimentation coefficent, s	1.6	2.9	3.9	5.8	8	9.9	13.4	16.8	19.9	23.3
Oligomerization state from s	fragments? **14.2%**			monomer	dimer	trimer	tetramer?			
Molar mass, kDa	20	47	74	136	215	289	496	666	860	1085
Mass fraction, %	7.8	3.7	2.7	73.6	5.7	3	1.1	1	0.7	0.7
R_H, nm	3.1	4.1	4.8	5.9	6.8	7.5	9	10	10.9	11.7

3.3.5. Size-Exclusion High Performance Liquid Chromatography

SE-HPLC was conducted on the 4h UV-irradiated aggregate sample. Two samples were run and each sample was run with two replicates. An example chromatogram can be seen in Figure 40. The results from the runs are summarized in Table 14.

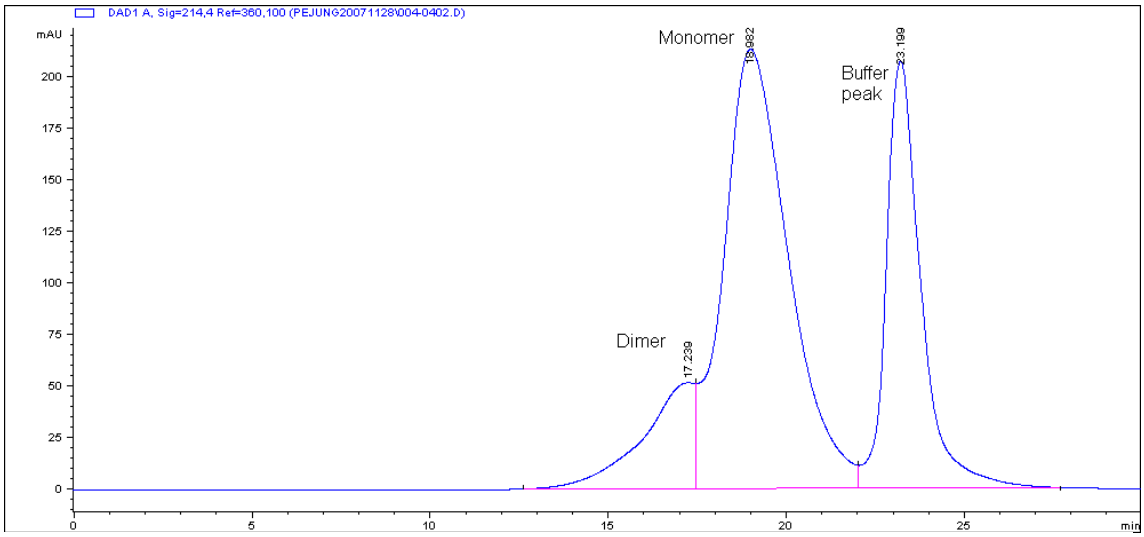

Figure 40. *SE-HPLC chromatogram of the 4h induced aggregate sample. The shoulder on the main peak are the aggregates, the main peak consists of both monomer and low molecular weight species, and the last peak is simply a system peak from the buffer used.*

Table 14*. Compiled results from the SE-HPLC runs.*

	Aggregate [area %]	Monomer [area %]
Sample 1:1	16,1	83,9
Sample 1:2	16,3	83,7
Sample 2:1	16,4	83,6
Sample 2:2	16,3	83,7
Mean	**16,3**	**83,7**

SE-HPLC is almost always the tool used for standard aggregate analysis of protein batches. The technique is usually very robust and easy to use once a method has been set up. In this analysis of a complex mixture it was hard to overcome interaction effects with the column matrix. These effects tend to break up the monomer peak due to unwanted secondary interactions with the gel in the column. However, this method has been qualified and therefore the values measured can be regarded as “true” values.

3.3.6. Correlation Study Results

Only data from A4F, SE-HPLC and SV-AUC will be compared since neither DLS nor native PAGE gave any comparable results. A comparison between the new optimized A4F method and the available qualified SE-HPLC method can be seen in Table 15. Here it is clear that the A4F method shows a significantly higher relative amount of aggregate than SE-HPLC. Only 75.5 % of the aggregates detected with A4F is detected with SE-HPLC.

A common opinion is that SE-HPLC might under-estimate the sample aggregate amounts since the molecules are subjected to high shear stress while passing the column and therefore might dissociate. This and other mechanisms of aggregation and dissociation has been outlined by Arakawa *et al* (2006). Another common opinion is that A4F might over-estimate the aggregate amount in the original sample because of the high sample concentrations induced by high crossflows and during the focusing step. In this case however, most of the aggregates in the sample are probably covalently cross-linked due to the UV-irradiation. This

means that very few aggregates should be lost in the SE-HPLC column. As for A4F the aggregate content was studied thoroughly in a DoE trial. Even though a model was fitted the impact of different parameters were low, often contrary to expectations, and could be well explained by measurement difficulties. Therefore, none of the opinions are likely to explain the measurement ratio as depending on real, although created, differences. The difference is therefore likely to depend on the accuracy of the actual method. What doesn't show either is that the A4F method was able to separate LMW impurities, which was not possible with the SE-HPLC method.

	A4F Dimer peak [%]	SE-HPLC Dimer peak [%]	Ratio SE-HPLC/A4F [%]
4h UV-irradiated antibody mixture	21.6 (n=2)	16.3 (n=4)	75.5

A previous study done in-house at Biovitrum compares the results from A4F with SE-HPLC and AUC, see Table 16. Here the sample is non-covalently aggregated. The A4F method used was however not the optimized method. In this study the SE-HPLC method is more sensitive to aggregates than the, not optimized, A4F method. It can be seen though that AUC, which is often referred to as the "gold-standard" in aggregate measurements, reports significantly higher amounts of aggregate than either A4F or SE-HPLC.

Table 16. *Results from in-house comparison of A4F, SE-HPLC and AUC. AUC shows a significantly higher aggregate amount than both A4F and SE-HPLC. For both A4F and AUC the presence of LMW species have been included in the Main peak since SE-HPLC cannot resolve these.*

	A4F Main peak [%]	SE-HPLC Main peak [%]	AUC Main peak [%]	Ratio SE-HPLC/A4F [%]	Ratio SV-AUC/A4F [%]
Un-aggregated sample	100	99.4	93.4	99.4	93.4
Non-covalently aggregated sample 1	100	97.2	88.9	97.2	88.9
Non-covalently aggregated sample 2	97.1	95.3	87.8	98.1	90.4
Average ratio:				98.2	90.9

3.4. Additional Experiments

3.4.1. Method Qualification

An example of an application of A4F is as an independent technique for qualification. The purpose of this experiment was to qualify an SE-HPLC method. In order to do this two samples were analyzed. One is a fully purified sample of an Fc-coupled protein. The other sample is taken prior to a final purification step and has a large content of Fc-tetramers.

An advantage with A4F is that it is very easy to achieve a fairly good separation. A4F is also very powerful when coupled to Refractive Index (RI) and Multi-angle Light Scattering (MALS) detectors for molecular weight determination. In only seven runs it was possible to

achieve a good separation of the samples and also to identify the peaks by mass determining the peak components. An overlay of the chromatograms with the estimated molecular masses can be seen in Figure 41 and the compiled data can be seen in Table 17.

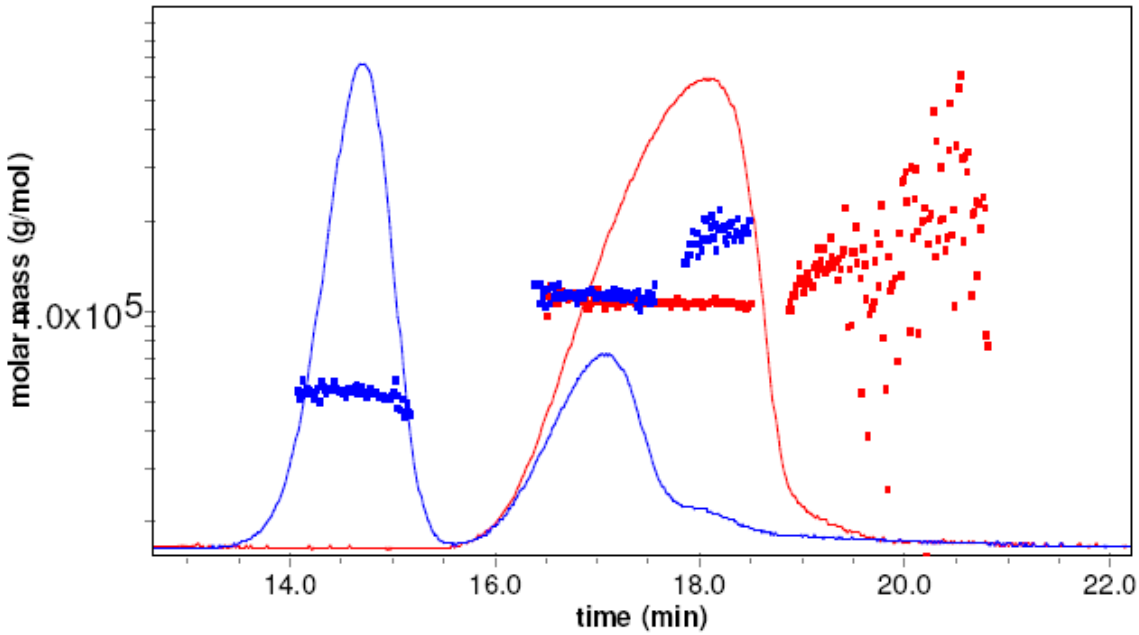

Figure 41. *Overlay of the fully purified (red) and the partly purified (blue) sample. A low molecular weight impurity, probably Fc tetramers, is detected in the partly purified sample but is completely lacking in the red. The molecular mass of the impurity is estimated to 54 kDa and it is designated peak 1. Peak 2 is the Fc-coupled protein main peak which is estimated to 114 and 108 kDa respectively. In both samples a small shoulder is detected on the main peak. This is designated peak 3 and its average mass is determined to 150 and 175 kDa. To detect possible high molecular weight impurities an area right after peak 3, before the signal returned to the baseline, was detected and quantified as peak 4. Note that for the purified sample the peaks following the main peak have been shifted to the right as compared with the blue sample.*

Table 17. *Summary of chromatogram results.*

Partly purified Fc-coupled protein

	Peak 1	Peak 2	Peak 3	Peak 4
Area %	61,8%	33,3%	3,8%	1,1%
Mol mass	54 kDa	114 kDa	175 kDa	300 kDa

Fully purified Fc-coupled protein

	Peak 1	Peak 2	Peak 3	Peak 4
Area %		97,3%	2,1%	0,7%
Mol mass		108 kDa	150 kDa	180 kDa

3.4.2. Stressed Conditions Aggregation

The UV/RI/MALS combination of detectors can, as was also seen in the previous study, be quite informative. Here an Fc-coupled protein sample was run in different elution buffers with different pH, see Figure 42 and 43.

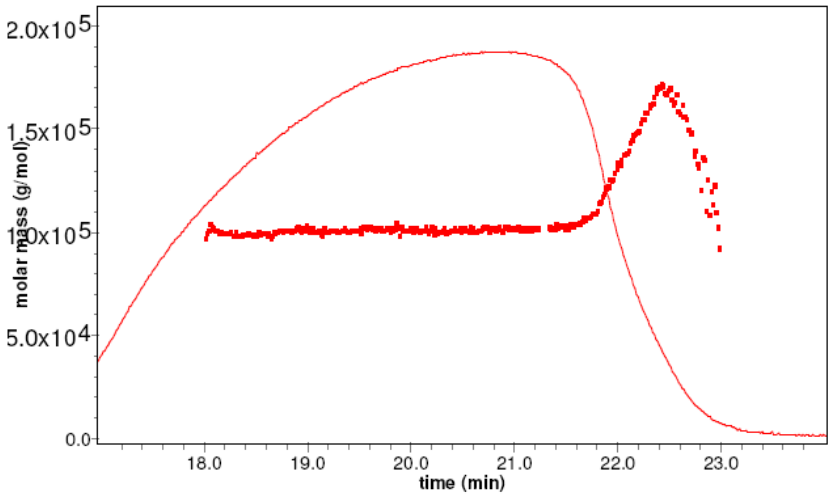

Figure 42. *Fc-coupled protein sample run at pH 7.5. Molecular weight of main peak estimated to ~100 kDa.*

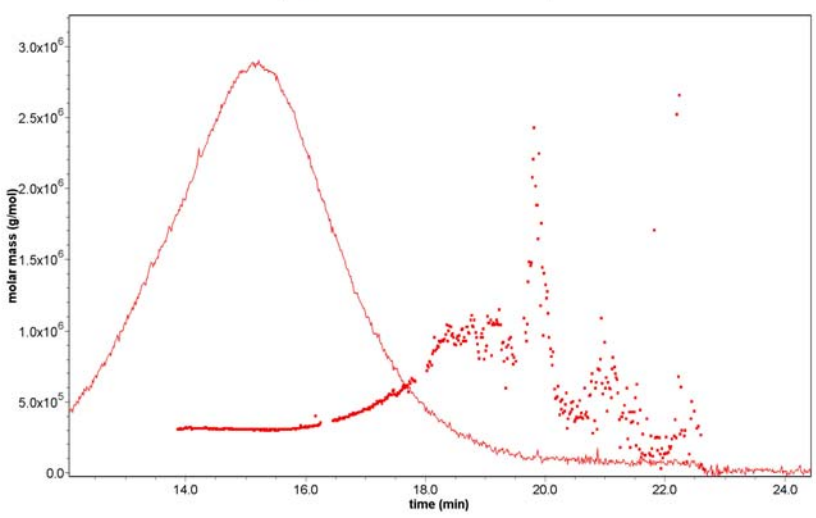

Figure 43. *Fc-coupled protein sample run at pH 3.5. Molecular weight of main peak estimated to ~320 kDa.*

Even though the peaks are not very sharp the molecular weight is well determined. The results clearly indicate that at low pH the sample forms trimers. This is interesting because the Fc-coupled protein can be purified with a protein A-column from which they are usually eluted in a low pH environment.

3.4.3. Separation of Pegylated Proteins

This experiment originates in difficulties of separating a pegylated protein on a SE-HPLC column. The purpose of the experiment was to determine whether a pegylation reaction had been successful or not. The UV-detector indicated that any protein in the sample eluted in the column void volume. Since it was not possible to separate the sample on SE-HPLC, A4F was employed to give it a try.

In four runs an acceptable elution assay had been developed. The chromatogram, see Figure 44, show a few peaks eluting with little or no retention, indiscriminable from the void volume. But also a large split peak eluting at 13 to 18 min – 5 to 10 minutes after the start of the gradient. With the assay employed this position, for a protein, would indicate a size of several hundred kDa. This would be way larger than expected. However, with the UV280/RI/MALS combination of detectors it is possible to determine both the PEG and the protein content in a peak.

To determine the mass a dn/dc value of 0.156 was calculated for a single coupled pegylated protein. Although the mass determinations are not very precise, they are in a range that would indicate a single protein coupled to a single PEG chain. The molecular mass of this complex is quite low when considering the position at which they elute. This, however, only demonstrates the basis of separation in A4F. As you would recall, the basis for the technique is the proteins diffusion coefficient, which is directly linked to its hydrodynamic radius. A pegylation tail on a protein forms a hydrodynamically very large compound. Actually, one of the main points of pegylating drug compounds is that their apparent large size prolongs their half-life by slowing down their renal clearance speed.

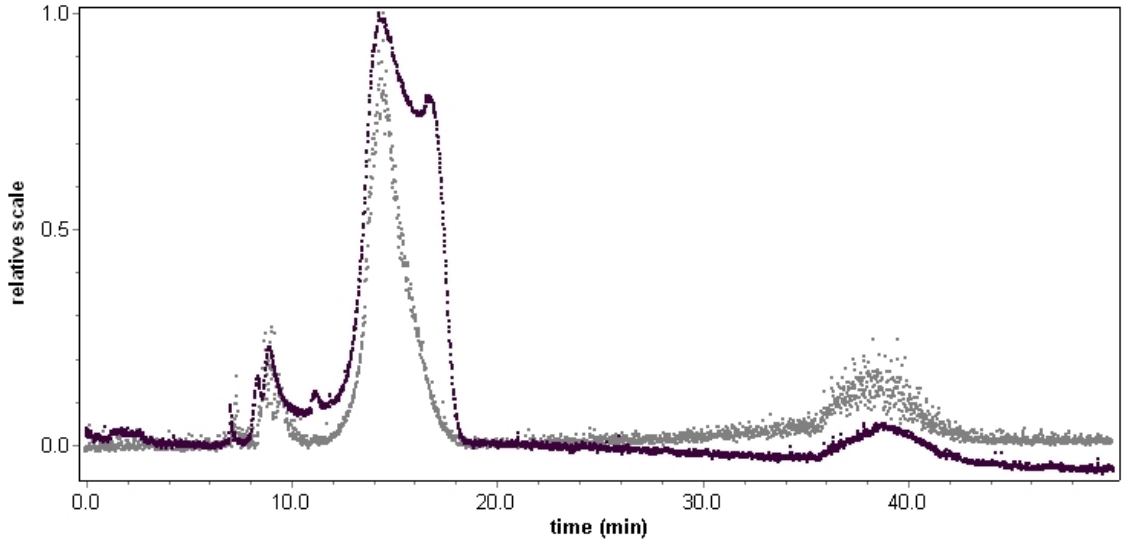

Figure 44. *Pegylated protein separation. UV280 (black) and 90 degrees LS (grey) detectors. Peaks before 10 min can be considered as void. Late flat peak elutes after flush-out has started.*

3.4.4. Long versus Short Channel Comparison

Wyatt Technology Europe has recently introduced a new channel design to its A4F system. The only previously available channel had a channel length of 267 mm tip to tip. The new

short channel has a length of 174 mm. Theoretically, the retention time shouldn't be affected by the channel length if the channel flow and the Vx/Vc ratio are constant. However, the shorter channel was said to give sharper peaks.

The performance of the Long and Short A4F channels was compared whilst using BioRad Gelfiltration Standard as analyte. BioRad GF consists of proteins ranging in size from 1.35 kDa to 670 kDa, see Table 18.

Table 18. *BioRad Gel Filtration Standard components.*

Protein	Mw [kDa]
Vitamin B12	1.35
Equine myoglobin	17
Chicken ovalbumin	44
Bovine gamma-globulin	158
Thyroglobulin	670

Elution schemes for both channels were developed and optimized in several runs. The development was done mostly on the long channel and thereafter the parameters were scaled down to give comparable separations. The final parameters for the different channels are listed in Table 19 below.

Table 19. *Optimized elution schemes for a BioRad GF separation on a long and a short A4F channel respectively.*

Long Channel

Flowrate:	1 ml/min	**Spacer:**	350M		**Sample Load:**	4 ug
Step	**delta t**	**Time**	**Mode**	**X start**	**X end**	**Focus Flow**
1	3.00	3.00	Elu	5.00	5.00	-
2	2.00	5.00	Focus	-	-	2.00
3	3.00	8.00	Foc+Inj	-	-	2.00
4	2.00	10.00	Focus	-	-	2.00
5	30.00	40.00	Elu	5.00	2.50	-
6	10.00	50.00	Elu+Inj	0.00	0.00	-

Short Channel

Flowrate:	0.8 ml/min	**Spacer:**	350M		**Sample Load:**	4 ug
Step	**delta t**	**Time**	**Mode**	**X start**	**X end**	**Focus Flow**
1	3.00	3.00	Elu	4.00	4.00	-
2	2.00	5.00	Focus	-	-	2.00
3	3.00	8.00	Foc+Inj	-	-	2.00
4	2.00	10.00	Focus	-	-	2.00
5	30.00	40.00	Elu	4.00	2.00	-
6	10.00	50.00	Elu+Inj	0.00	0.00	-

The resulting chromatograms for the runs are presented in Figure 45 to 47.

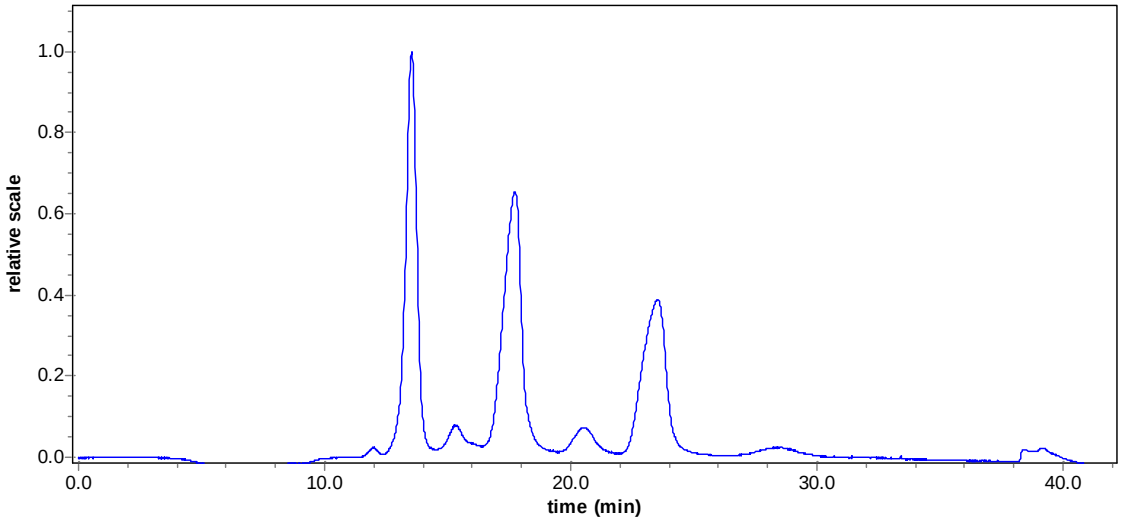

Figure 45. *Chromatogram for long channel.*

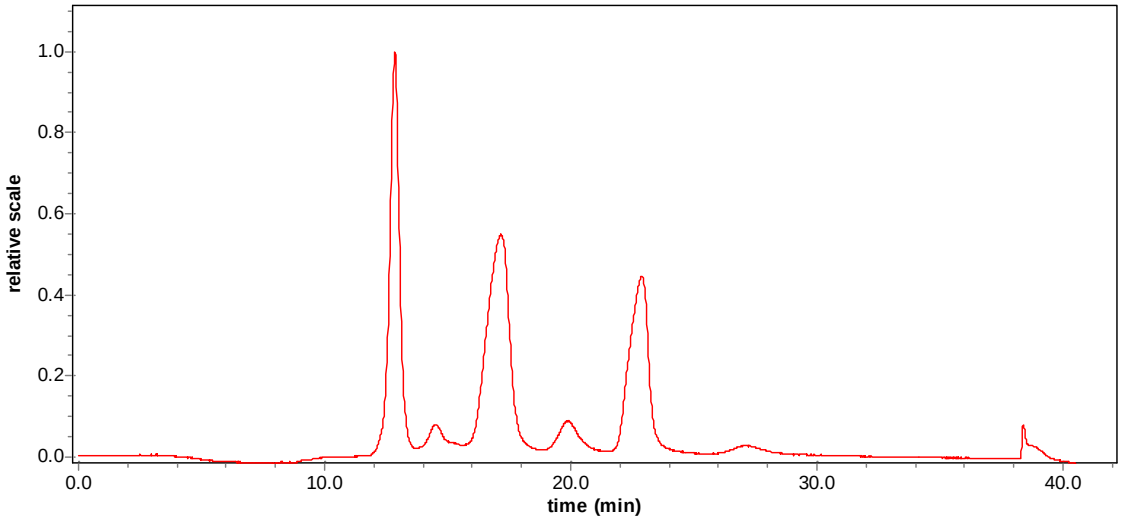

Figure 46. *Chromatogram for short channel.*

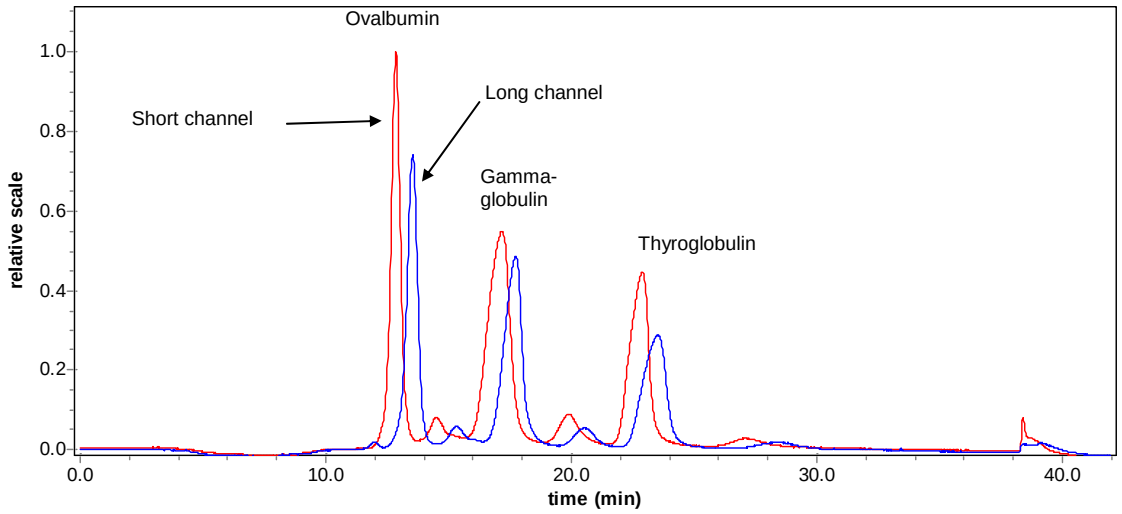

Figure 47. *Overlay of chromatograms. The red (with the highest peak) is for the short channel, and the blue for the long channel.*

The three main peaks correspond to ovalbumin, gamma-globulin and thyroglobulin, and the smaller peak following each main peak is most probably dimer species. The membrane used was a Regenerated Cellulose membrane with a 10 kDa nominal cut-off. This means that the 1.35 kDa vitamin was flushed out and not registered. However, one can note that also the 17 kDa myoglobin apparently passed through the membrane and didn't register.

The two runs had the same Vx/Vc-ratio. This theoretically means that they should have the same retention times. As can be seen though, the short channel elutes the peaks slightly prior to the long channel. A possible explanation is that the set crossflow for the small channel is borderline to what it can handle. This might have meant that the actual crossflow was a bit lower than set and, correspondingly, the channel flow a bit higher, which then resulted in a quicker elution.

The resolution is very good for both channels. No significant differences in peak width or resolution can be seen either way.

4. Conclusions

Both practical and theoretical conclusions are presented here. The conclusions are divided into five sections concerning different aspects of this study and also of the technique and the actual system used. The five sections deals with the optimized method, the correlation studies, method development parameters, general system characteristics and other practical considerations.

- In this study an optimized A4F method has been developed for a sample consisting of an antibody mixture. The method manages to separate LMW impurities, the main peak and aggregate species.

- Compared to an optimized SE-HPLC method, the A4F method is more sensitive for aggregates and can also detect and quantify LMW impurities which the SE-HPLC method cannot.

- Analytical ultracentrifugation is the most sensitive method to detect and quantify LMW impurities, main analyte and aggregate species. The high cost of AUC (around 15-30k SEK per sample) limits its applicability to mostly validating other methods.

- With A4F it is extremely easy to set up good separations for challenging macromolecular analyses. Until the system is better characterized and GMP-compliant, SE-HPLC will remain the work-horse for standard routine analyses though.

- For the heterogenous antibody mixture sample the un-optimized native PAGE method was not very informative.

- The extreme range of A4F makes it a possible candidate to complement DLS in analyses of large aggregates. DLS is not suited to discriminate between monomer/dimer species.

- The crossflow to channel flow ratio Vx/Vc was found to be the most influential parameter on the retention time, and therefore the most important separation parameter.

- Increasing the channel flow Vc while keeping the Vx/Vc ratio constant sharpens the peaks. However, membranes have a maximum Vx ratio so it is not possible to scale up Vx/Vc infinitely.

- Using a cross flow gradient usually gives sharper peaks and greater range. But when using a gradient the refractive index signal gets distorted by the pressure change. This makes it more difficult to use an RI/MALS combination to appreciate the size of the analytes.

- An increased sample load give broader peaks and also slightly displaces the peak maximum. For optimizing separations it is therefore recommended to use an as low

sample load as possible, while still maintaining an acceptable signal to noise level. However, mass determinations are more accurate with sufficiently high sample levels.

- In this study no significant impact on the separation was found with any specific membrane. The regenerated cellulose membrane was preferred however since it could be reused when changing to an equally or less wide spacer during screening. The polyethersulphone membrane stuck to the spacer and couldn't be reused.

- When choosing a membrane one also has to consider the pore size. A larger pore size can handle a larger crossflow. In this study membranes with 10 kDa cut-off was almost in-variably used and are probably appropriate for most protein separation tasks. 10 kDa is only a nominal value, however, myoglobin with a size of 17 kDa also passed through the pores.

- The focus time was not found to be a great factor in this study, an intermediate value of three minutes injection plus two minutes relax-time often seems appropriate.

- A high spacer give broader peaks but allows for a higher sample load. A thin spacer gives narrower peaks but a less stable system. 350 µm is a good compromise.

- The width of the spacer was not found to have any significant impact on separations. A wider spacer could possibly take more sample load. When using a high Vx/Vc ratio a more trapezoidal shaped spacer also help even out the varying flow ratio through-out the channel (consider the extremes: a trapezoidal channel with no crossflow has a higher flow velocity in the thin outlet end than in the inlet, where as a rectangular channel with high crossflow would have a high flow velocity at the inlet end).

- No significant differences were found between the long and the short channel. In this study the long channel was preferred because of more experience with this.

- No problems with carry-over between the runs were encountered.

- The system has a good reproducibility as studied between SSTs in a sequence. More experience is needed here though.

- More or less any sample can be well separated in a run time below 60 minutes.

- Sequential runs are possible and stable.

- After the change of a membrane it is necessary to condition the membrane by somehow saturating it by running a couple of samples. Two injections with around 15 µg protein has been sufficient to prevent subsequent sample loss. Independent of conditioning protein no carry-over has been noticed.

- Most elution buffers are good substrate for bacterial growth. Bacterial growth severely affect the noise in especially the MALS detector. To avoid bacterial growth the system has been left running in 20% ethanol overnight. This have had a positive effect on the

MALS data quality, both in preventing signal spikes and in keeping a low baseline. It is recommended to first flush the system with water before changing between saline buffers and ethanol to avoid crystallization of salts.

- When flushing the system one should remember internal dead volumes such as the sample injection loop and the channel compartment below the membrane. To flush also these one should remember to turn on a sample injection flow and a crossflow respectively.

- The refractive index signal is a good indicator of when the system has been equilibrated with a new buffer. This usually takes at least 15-30 minutes.

- A crucial component of the system is the LiquiFlow that splits the pump flow between channel flow and crossflow. This crucial component is reported not to work if the channel pressure is below 9 bar. The LiquiFlow is governed by a setting called the conversion factor. For the system at Biovitrum this setting should be 0.852 for PBS buffer. The setting is however dependent on the salinity of the buffer, so other buffers could have other settings.

5. Raw Data

Raw data from the experiments is stored in Biovitrum's electronic labnotebook system. Related ELN experiment numbers are EXP-07-DB9703, EXP-07-DB9704, EXP-07-DB9706, EXP-07-DB9710 and EXP-07-DB9711. Additional data, such as ASTRA and MODDE files is stored electronically according to internal routines at Biovitrum. They can be found on an archieved CD labelled "Per Jungnelius Examensarbete Datafiler 2008-02-22".

6. References

Agilent Technologies, *Agilent Chemstation – Understanding Your Chemstation*, Edition 04/00, **(2000)**, Agilent Technologies: Germany.

Arakawa, T., Philo, J. S., Ejima, D., Tsumoto, K. & Arisaka, F., 'Aggregation Analysis of Therapeutic Proteins, Part 1: General Aspects and Techniques for Assessment', *BioProcess International* **(2006)**, *4(10)*, 32-42.

Arakawa, T., Philo, J. S., Ejima, D., Tsumoto, K. & Arisaka, F., 'Aggregation Analysis of Therapeutic Proteins, Part 2: Analytical Ultracentrifugation and Dynamic Light Scattering', *BioProcess International* **(2007)**, *5(4)*, 36-47.

Eriksson, L., Johansson, E., Kettaneh-Wold, N., Wikström, C. & Wold, S., *Design of Experiments: Principles and Applications*, **(2000)**, Umetrics Academy: Umeå, Sweden.

Fraunhofer, W. & Winter, G., 'The Use of asymmetrical flow field-flow fractionation in pharmaceutics and biopharmaceutics', *European Journal of Pharmaceutics and Biopharmaceutics* **(2004)**, *58*, 369-383.

Gabrielson, J. P., Brader, M. L., Pekar, A. H., Mathis, K. B., Winter, G., Carpenter, J. F. & Randolph, T. W. 'Quantitation of Aggregate Levels in a Recombinant Humanized Monoclonal Antibody Formulation by Size-Exclusion Chromatography, Asymmetrical Flow Field Flow Fractionation, and Sedimentation Velocity', *Journal of Pharmaceutical Sciences*, (**2007)**, *96(2)*, 268-279.

Litzén, A. & Wahlund, K.-G., 'Zone Boadening and Dilution in Rectangular and Trapezoidal Asymmetrical Flow Field-Flow Fractionation Channels', *Analytical Chemistry* **(1991)**, *63*, 1001-1007.

Markova, N., 'AUC sedimentation velocity study of three [...] samples', confidential report, **(2007)**.

Wahlund, K.-G. & Giddings, J. C., 'Properties of an Asymmetrical Flow Field-Flow Fractionation Channel Having One Permeable Wall', *Analytical Chemistry* **(1987)**, *59*, 1332-1339.

Walker, J. M., 'Chapter 10. Electrophoretic techniques' in Wilson, K. & Walker, J. (ed.), *Principles and Techniques of Biochemistry and Molecular Biology, 6th Ed*, **(2005)**, Cambridge University Press.